Avaliação Quantitativa Ultrassônica de Estruturas de Concreto

Professor Lev Khazanovich
Dr. Kyle Hoegh

U.S. Department of Transportation
Federal Highway Administration

SHRP2
STRATEGIC HIGHWAY RESEARCH PROGRAM

MINNESOTA DEPARTMENT OF TRANSPORTATION

DEPARTMENT OF ENERGY · UNITED STATES OF AMERICA

Outline

- Introduction
  - Active elastic wave-based methods
  - Conventional data interpretation methods
  - Linear array ultrasound systems
- Linear array signal reconstruction and interpretation
- Applications
  - Concrete thickness
  - Reinforcement location
  - Damage assessment
- Conclusions

Wave Propagation/Reflection

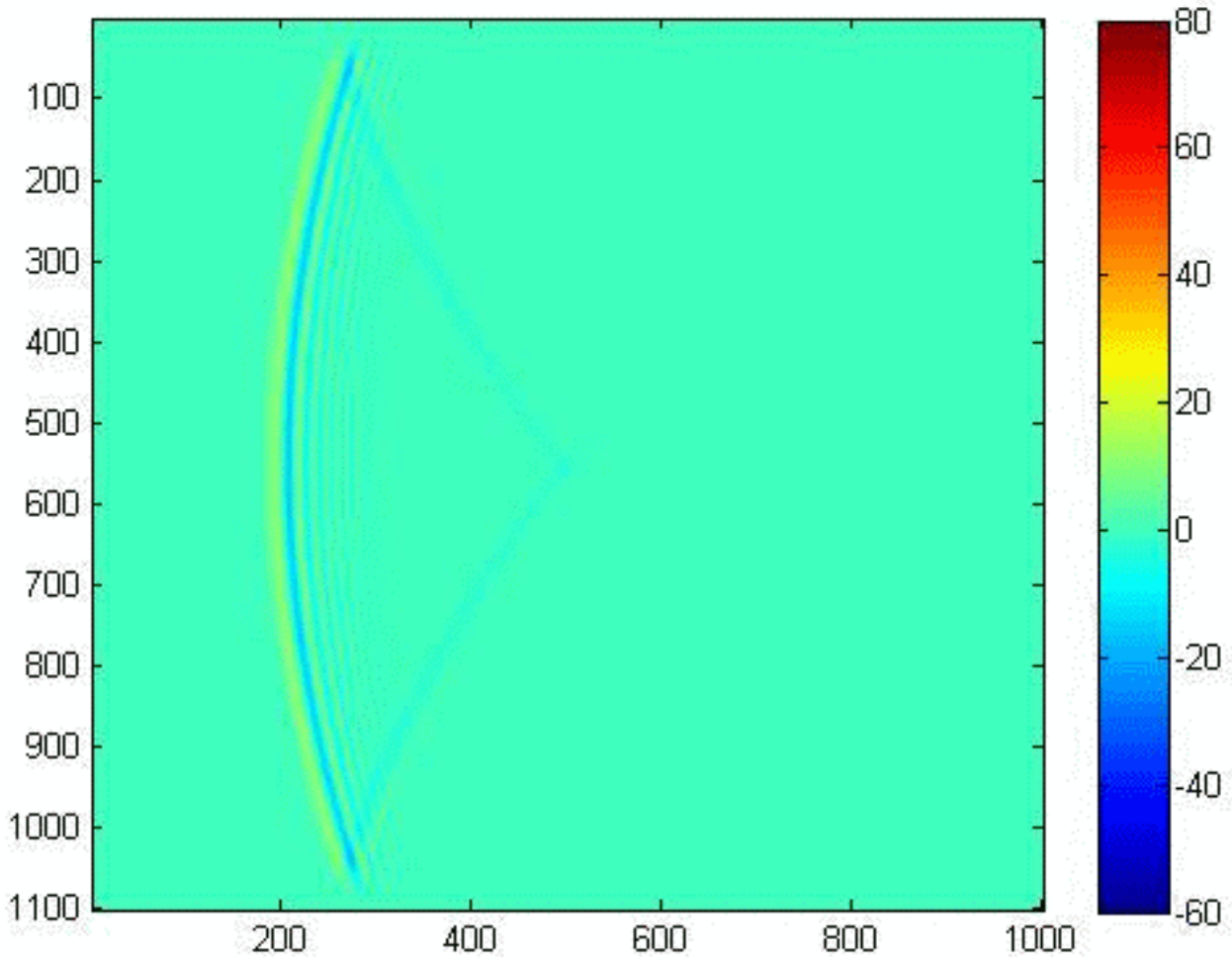

Active Elastic Wave-Based Methods

Chain and Rod Sounding

http://www.fhwa.dot.gov/pavement/concrete/repair04.cfm

Conventional Impact Echo

Proceqs Pundit

James NDT V-Meter

esy of Olson Engineering, Inc.

Ultrasonic Linear Array

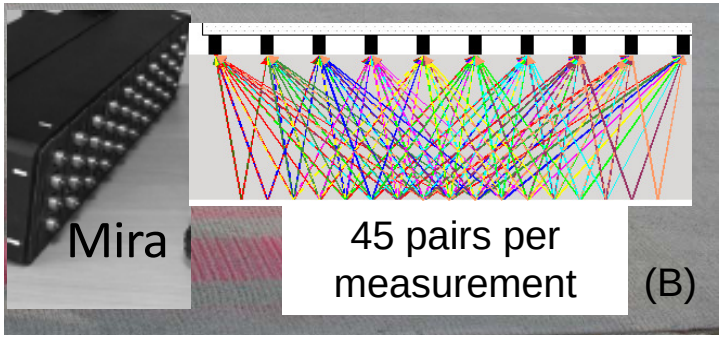

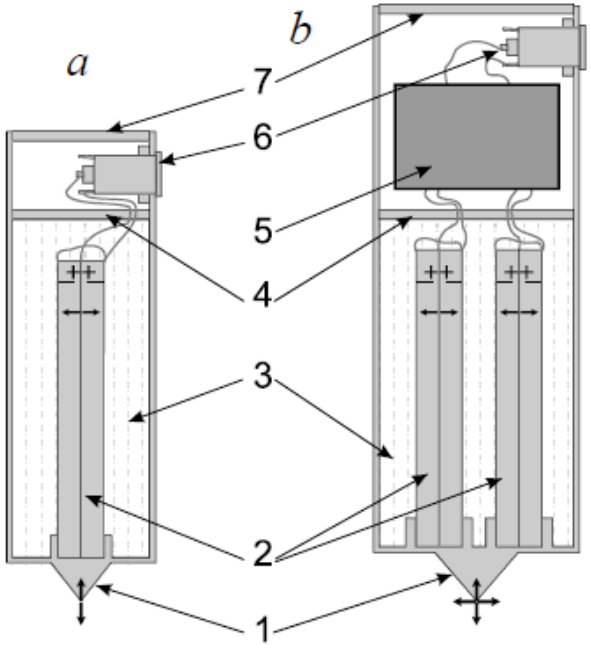

- Ponto Seco de Contato (DPC) – Transdutores de Baixa Frequência
  - Fabicado por Acoustic Control Systems, Ltd, Moscow, Russia
  - Não requer preparo da superfície
  - Aparelhos de toque e medida com alto grau de precisão
  - Os transdutores agem na supefície do objeto de teste com elementos de ocilação piezoelétricos para produção de ondas e captação de sinais
    - out of phase for s-wave production
    - in phase for p-wave production

- Representação Convencional
  - A-scans
  - B-scans
- Reconstrução de Métodos
  - Abertura instantânea técnica de abertura focal sintética (SAFT)

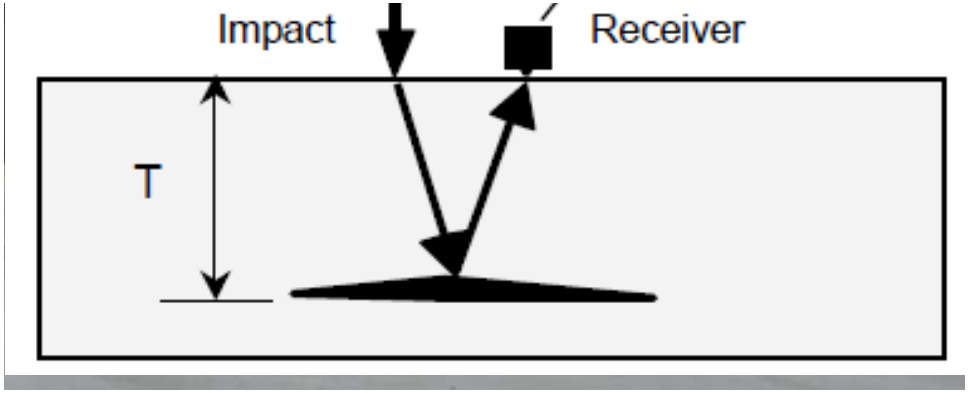

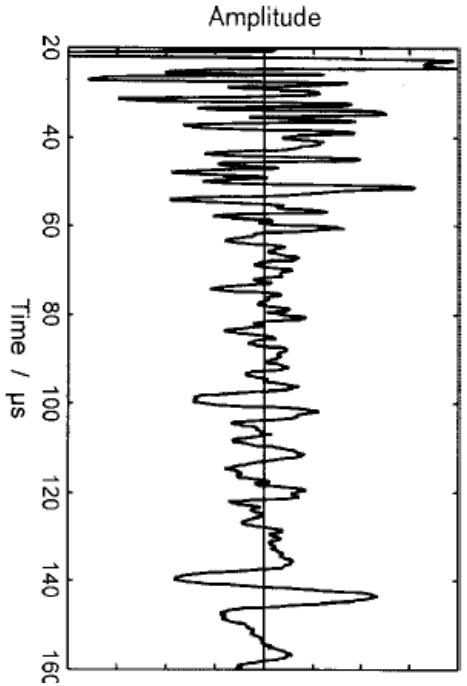

$$t = \frac{2z^*}{c}$$

Schickert et al., 2003

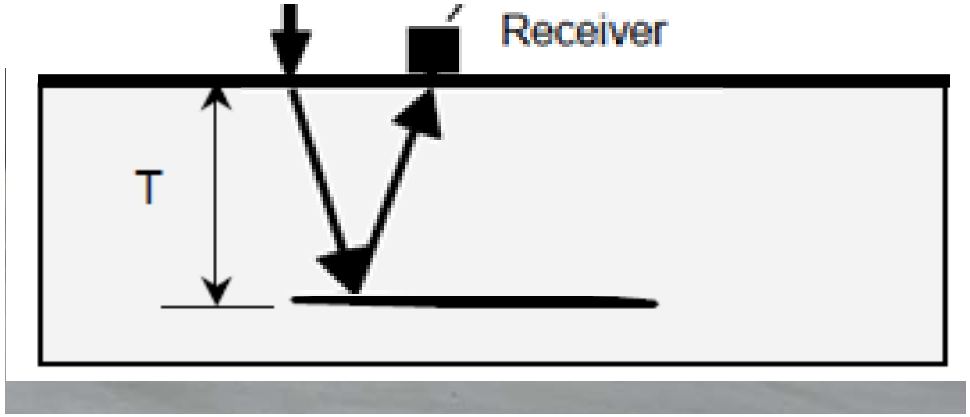
Receiver
T

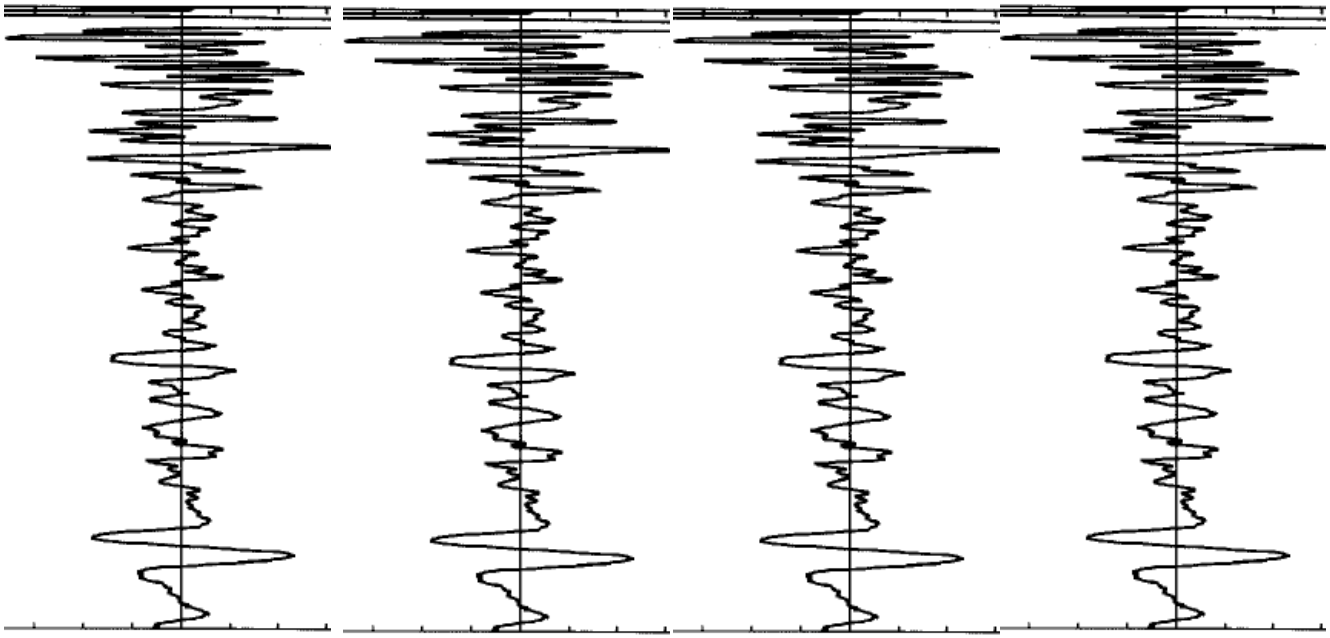

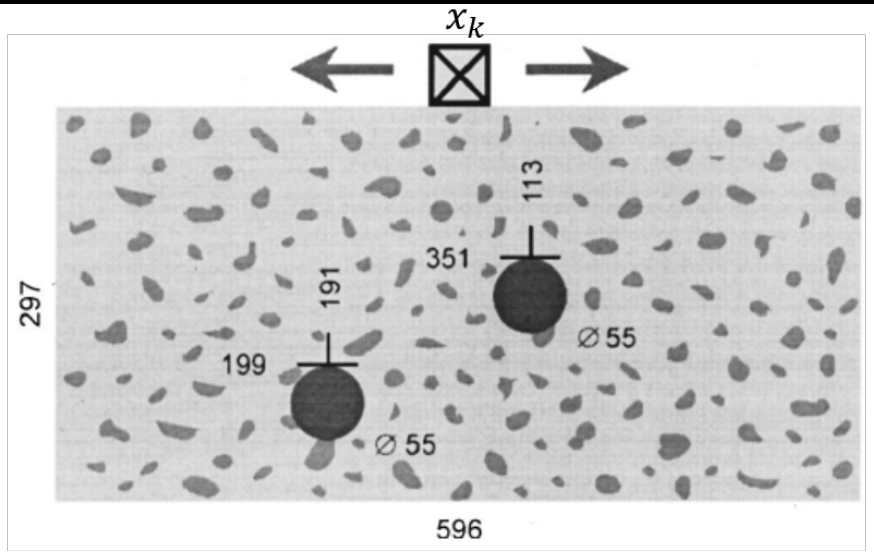

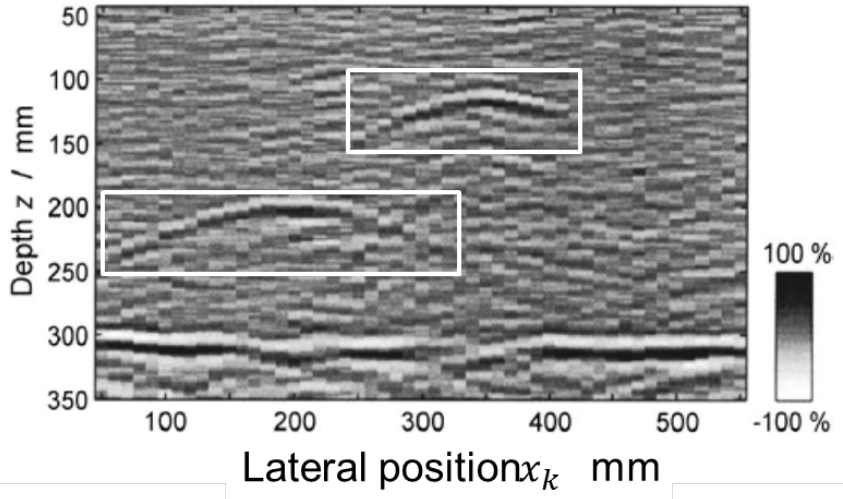

Schickert et al., 2003

$$s(x_k, t) = \int_x \cdot \int_z \cdot f(x, z)\delta(t^*(t, x_k, x, z))dzdx$$

Onde $s(x_k, t)$ é o estímulo recebido na posição do transdutor, x_k, devido ao pulso emitido $\delta(t^*(t, x_k, x, z))$; $f(x, z)$ é a função de reflexão de ROI; x e z são as coordenadas horizontal e vertical em ROI, respectivamente

t^* é definido pela seguinte relação:

$$t^* = t - \frac{2}{c}\sqrt{z^2 + (x - x_k)^2}$$

Bamler 1992

Reflection Coefficient, R

$$\Psi_R = \frac{C_{s_1}\rho_1 - C_{s_2}\rho_2}{C_{s_1}\rho_1 + C_{s_2}\rho_2}\Psi_I = \frac{Z_1 - Z_2}{Z_1 + Z_2}\Psi_I = R_{1,2}\Psi_I$$

Kirchhoff Migration

$$t^* = t - \frac{2}{c}\sqrt{z^2 + (x - x_k)^2}$$

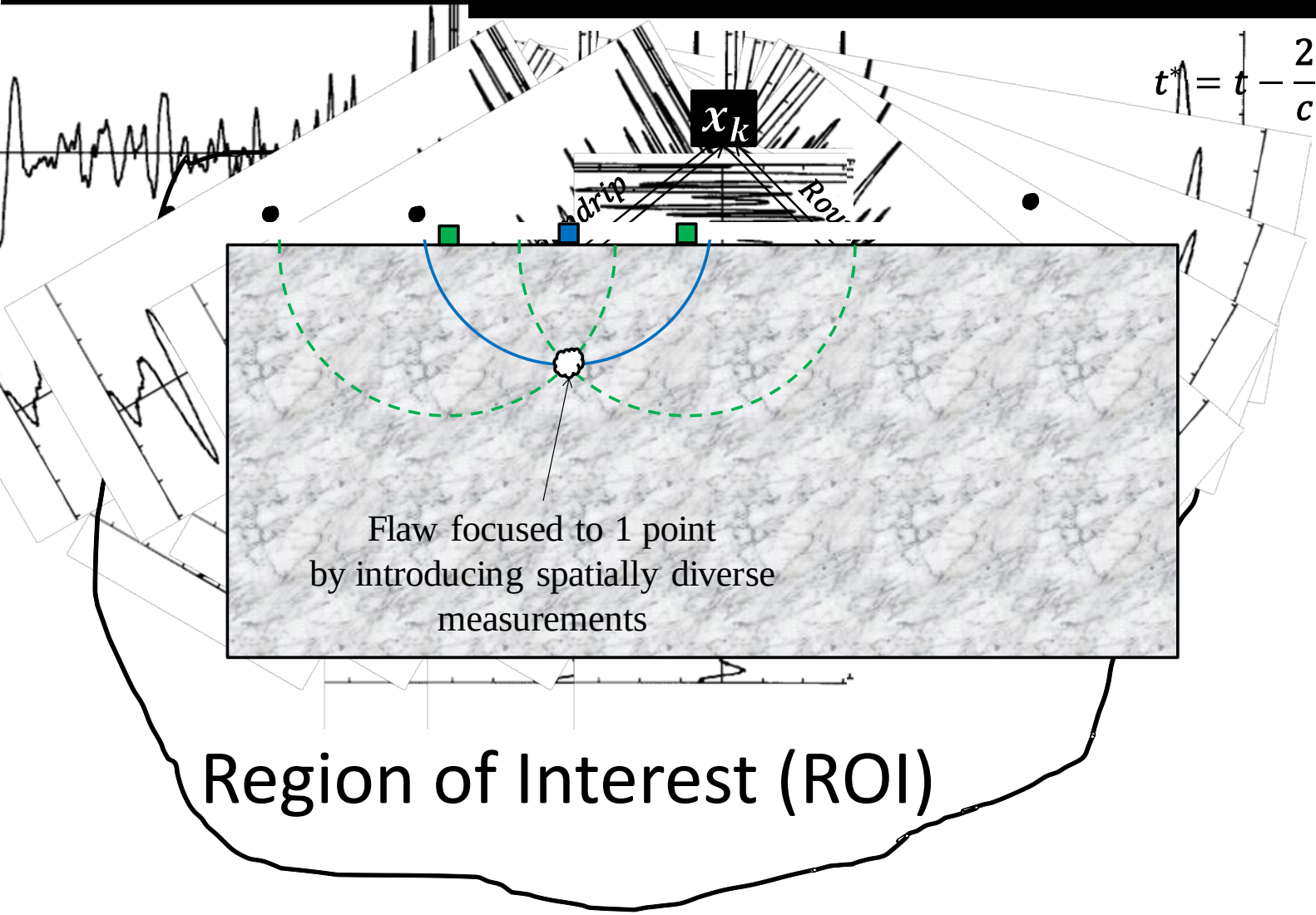

Region of Interest (ROI)

B-Scan vs Kirchhoff Migration

B-SCAN

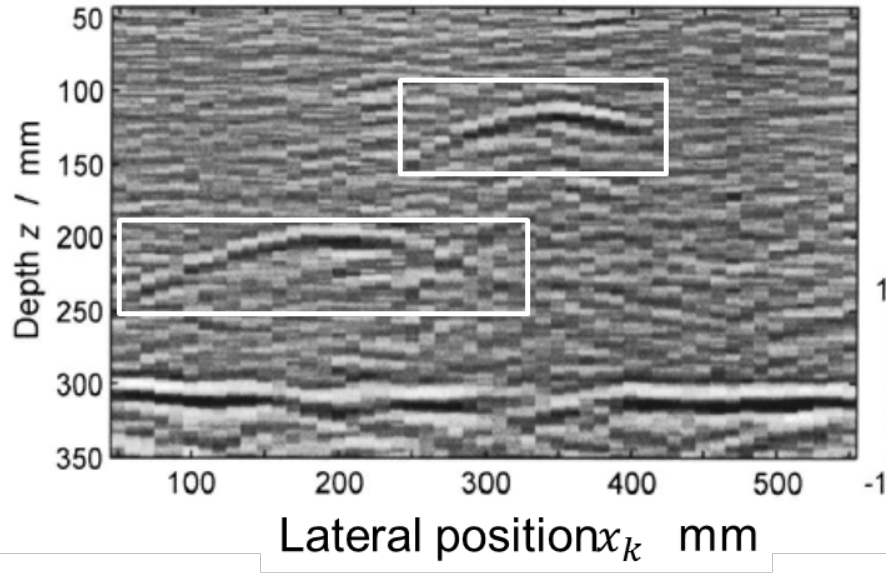

Kirchhoff Migration or
Synthetic Aperture Focusing Technique (**SAFT**)

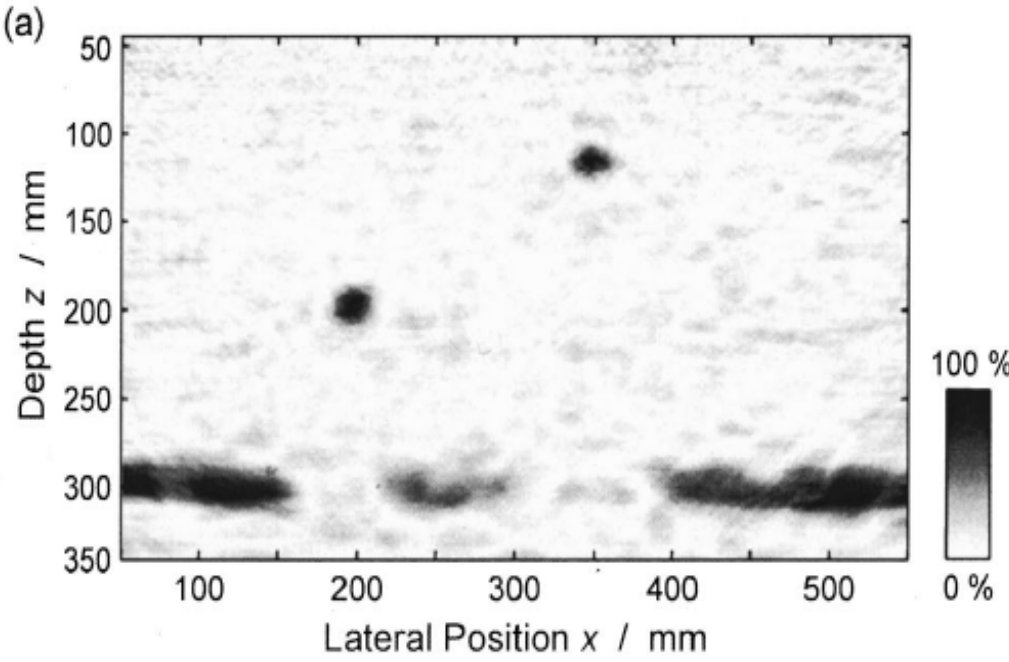

Schickert et al., 2003

Ultrasound Array Data

Histórico de Impulso de Onda de Cisalhamento

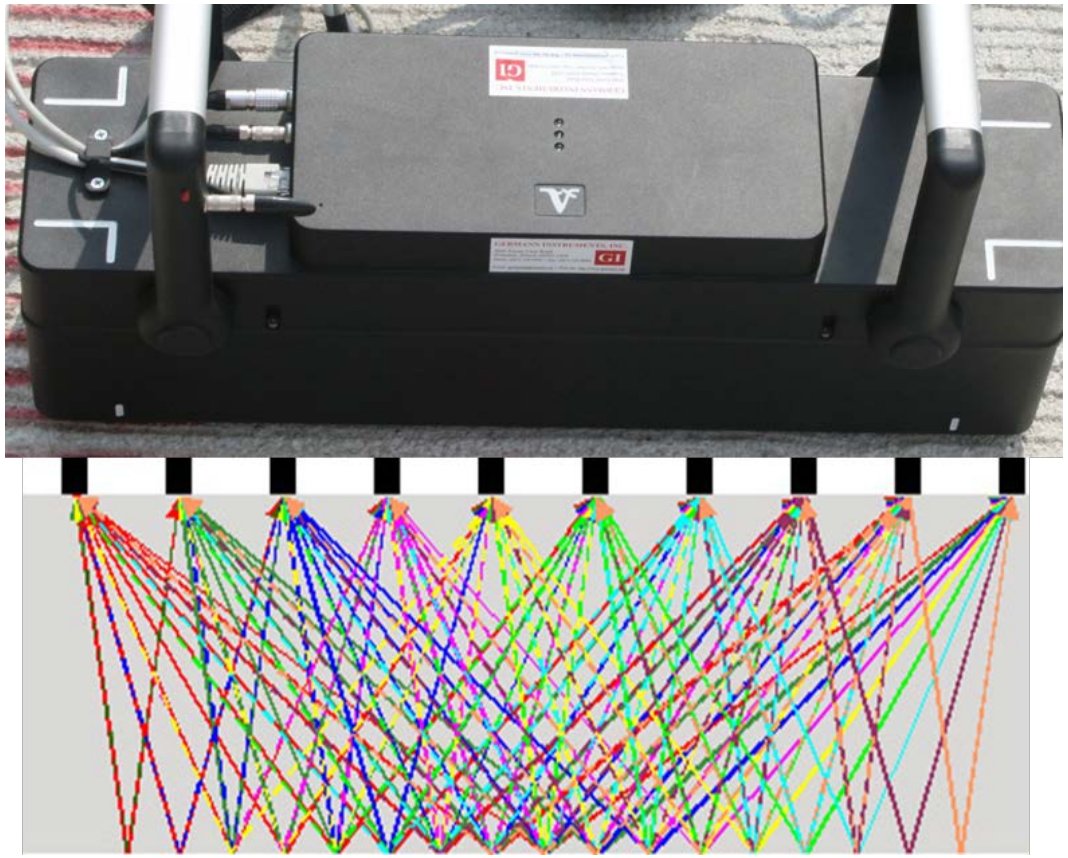

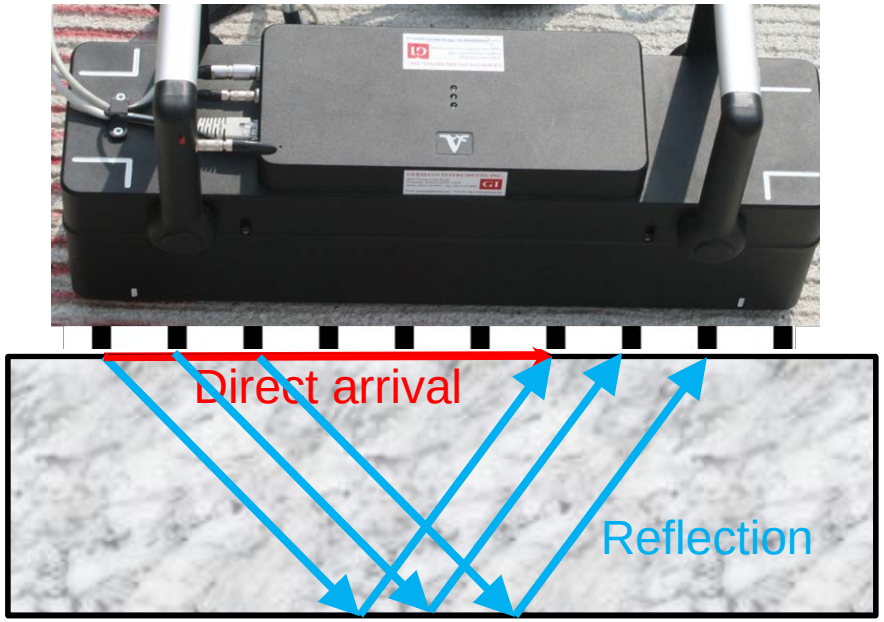
Direct arrival
Reflection

A-Scan

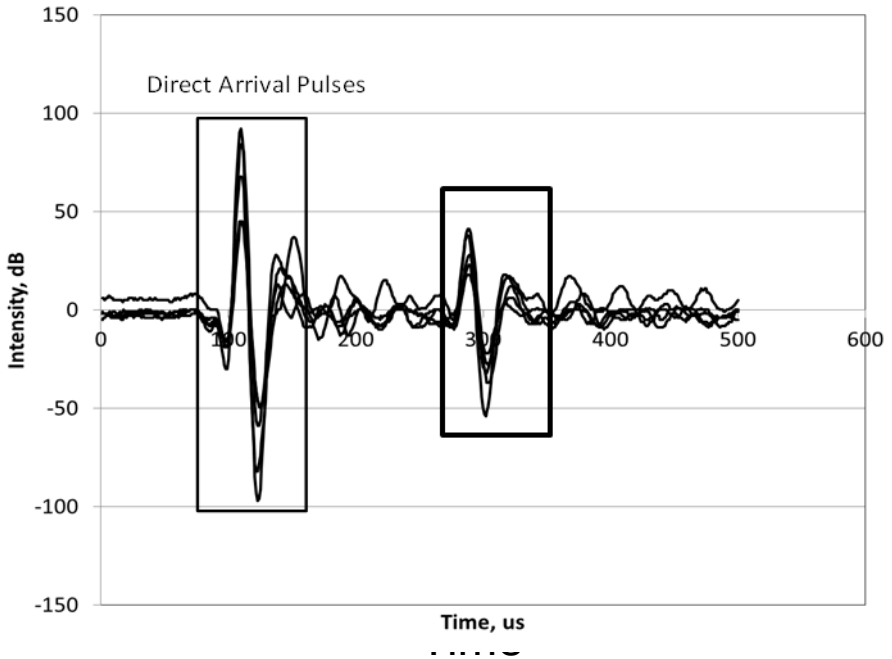
Direct Arrival Pulses
Intensity, dB
Time, us
150
100
50
0
-50
-100
-150
0
100
200
300
400
500
600

Histórico de Impulso de Onda de Cisalhamento

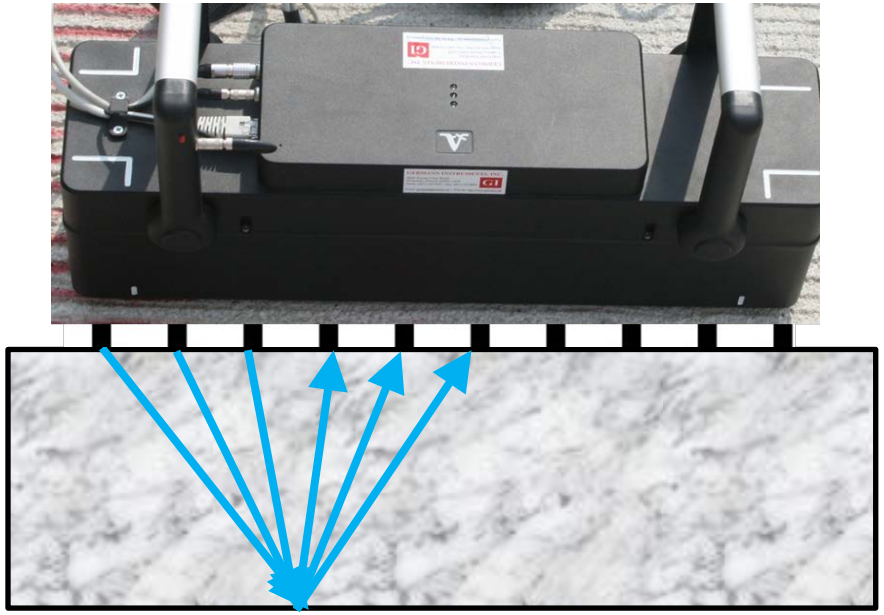

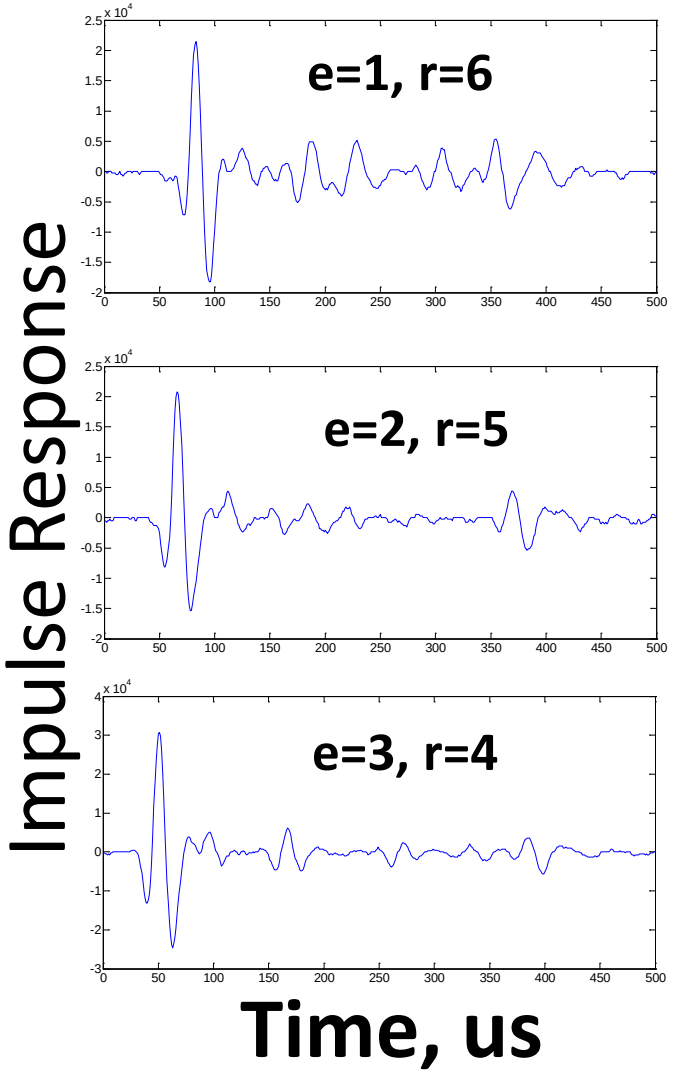

Time to Space Domain

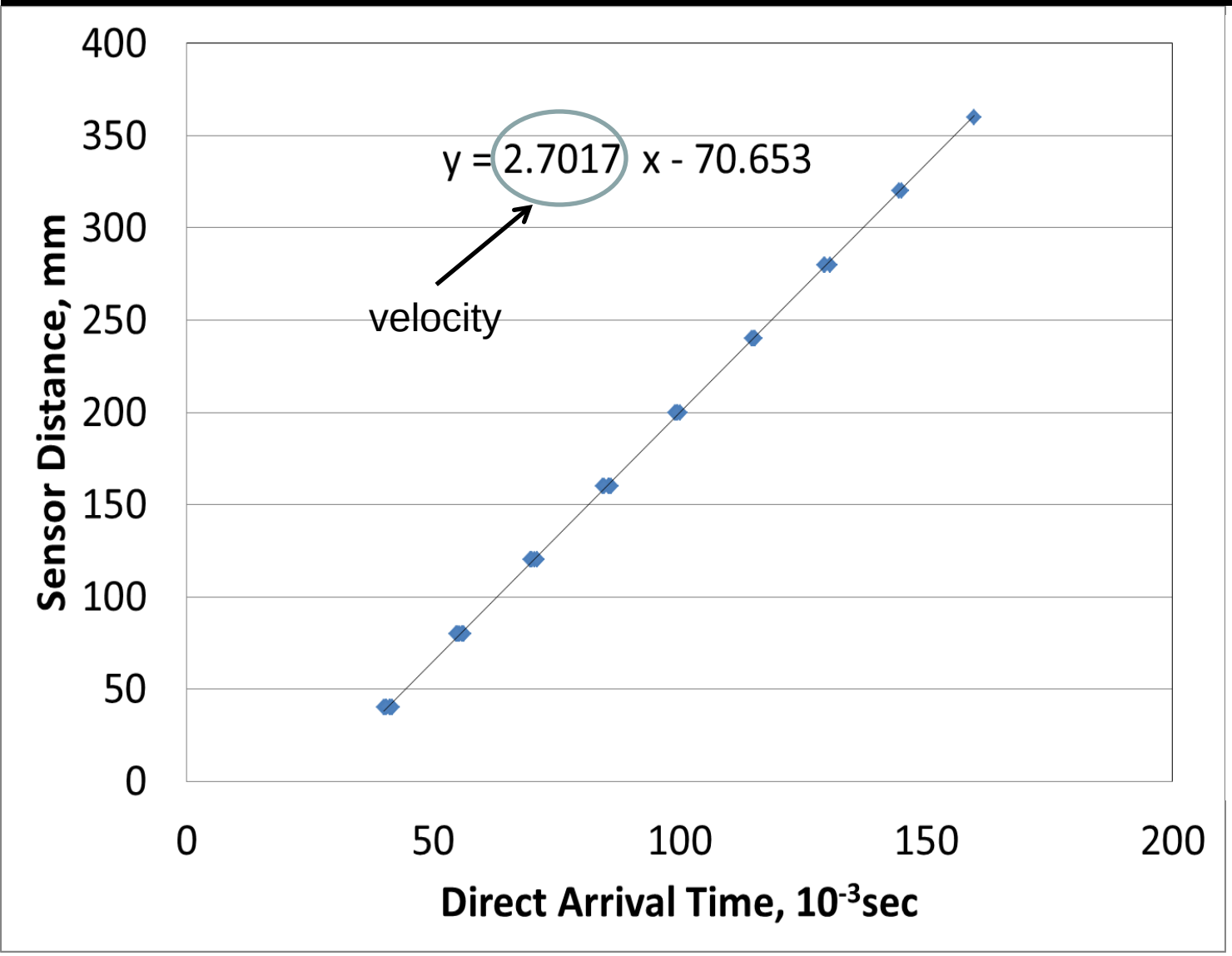

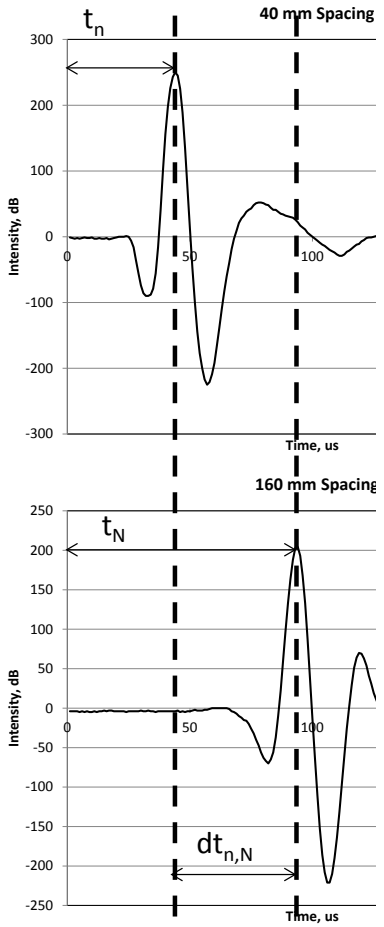

Matriz Linear
Reconstrução de Sinal e Interpretação

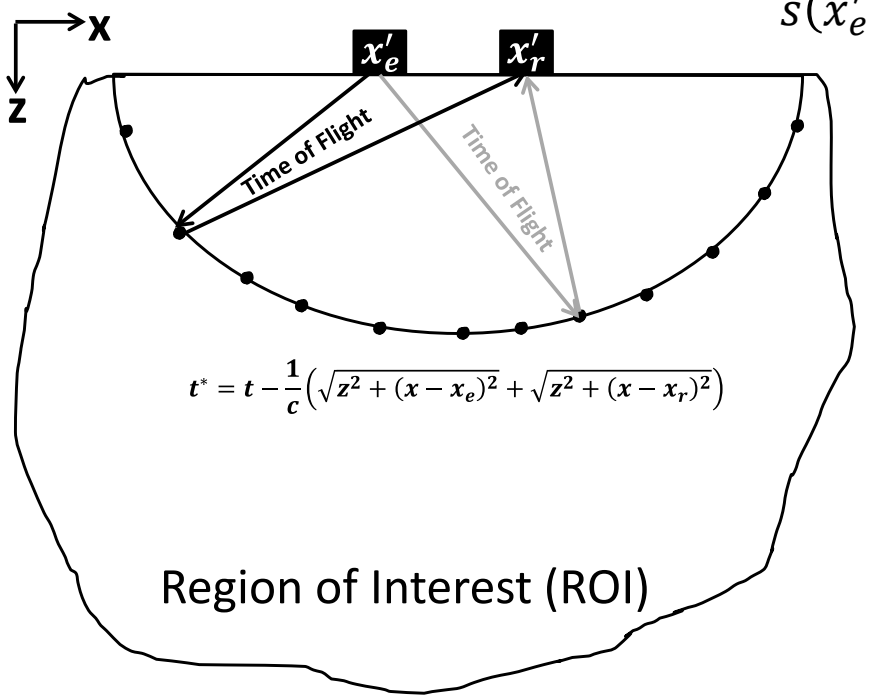

$$s(x'_e, x'_r, t) = \int_x \int_z f(x,z) * \delta(t^*(t, x'_e, x'_r, x, z))dzdx$$

$s(x'_e, x'_e, t)$ - Impluso recebido
$\delta(t^*(t, x'_e, x'_r, x, z))$ - Impulso emitido
$f(x,z)$ -Função da reflexão
ROI – Região de interesse com coordenadas horizontal e vertical, x e z

t^* é definido pela seguinte relação:

$$\Psi_R = \frac{C_{s_1}\rho_1 - C_{s_2}\rho_2}{C_{s_1}\rho_1 + C_{s_2}\rho_2}\Psi_I = \frac{Z_1 - Z_2}{Z_1 + Z_2}\Psi_I = R_{1,2}\Psi_I$$

$$t^* = t - \frac{1}{c}\left(\sqrt{z^2 + (x - x_e)^2} + \sqrt{z^2 + (x - x_r)^2}\right)$$

SAFT Discrete Spatially Diverse Pairs

$$\hat{o}(x,z) = \int_{x'_{emin}}^{x'_{emax}} dx'_e \int_{x'_{rmin}}^{x'_{rmax}} \mathrm{A}(x'_r, x'_e, x, z) * s\left(x'_r, x'_e, \frac{1}{c}\left(\sqrt{z^2 + (x - x'_e)^2} + \sqrt{z^2 + (x - x'_r)^2}\right)\right) dx'_r$$

Adaptado de Stepinski, 2007

$\mathrm{A}(x'_r, x'_e, x, z)$ é o fator de apodização; $\mathrm{A}(x'_r, x'_e, x_i, z_k) = \alpha_e(x'_e, x_i, z_k) * \alpha_r(x'_r, x_i, z_k)$

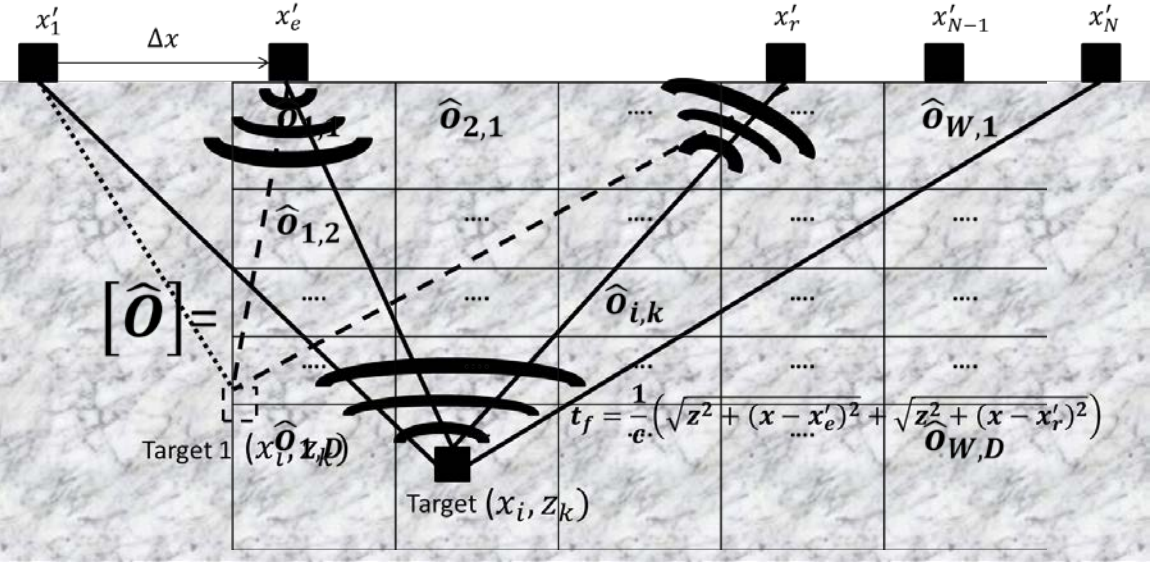

$$\alpha_e(x'_e, x_i, z_k) = \frac{z_k}{\sqrt{(x_i - x'_e)^2 + {z_k}^2}}$$

$$\alpha_r(x'_e, x_i, z_k) = \frac{z_k}{\sqrt{(x_i - x'_r)^2 + {z_k}^2}}$$

$$\hat{o}_{i,k} = \sum_{e=1}^{T-1} \sum_{r=e+1}^{T} \mathrm{A}(x_r, x_e, x_i, z_k) \Psi_{e,r}(x_i, z_k)$$

$$\Psi_{e,r}(x_i, z_k) = s\left(x_r, x_e, \frac{2}{c}\left(\sqrt{{z_k}^2 + (x_i - x_e)^2} + \sqrt{{z_k}^2 + (x_i - x_r)^2}\right)\right)$$

SAFT Discrete Spatially Diverse Pairs

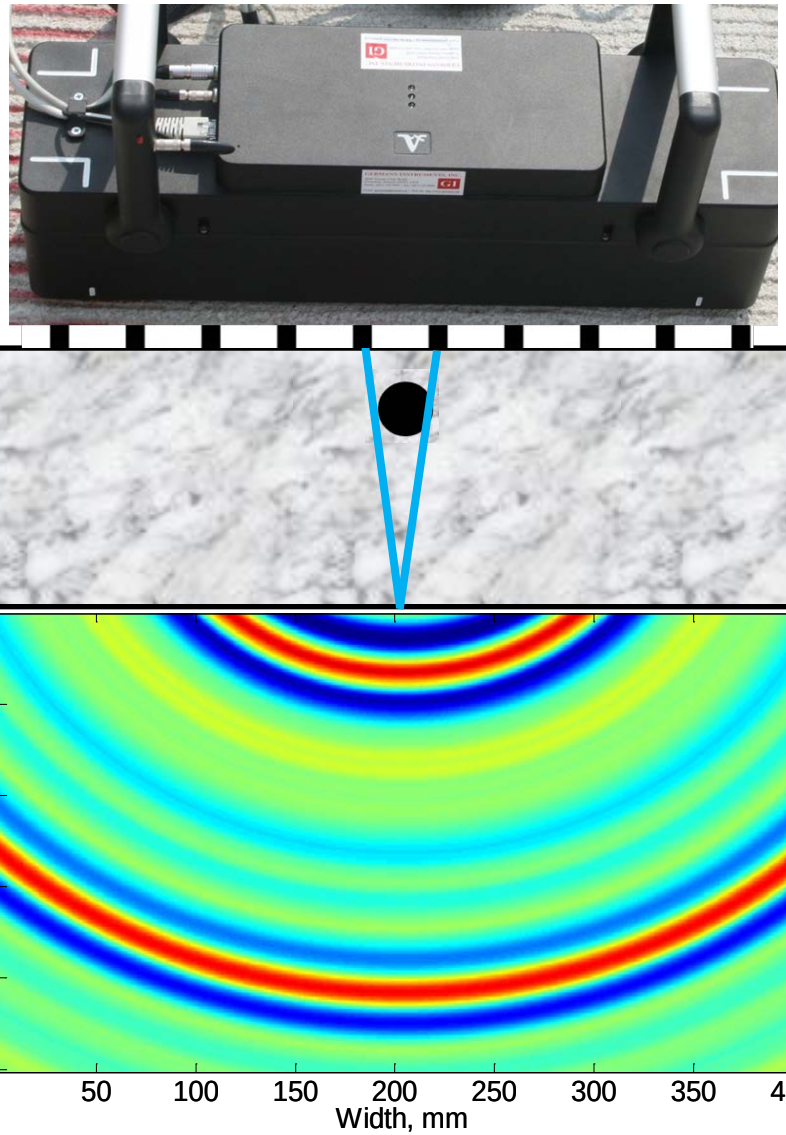

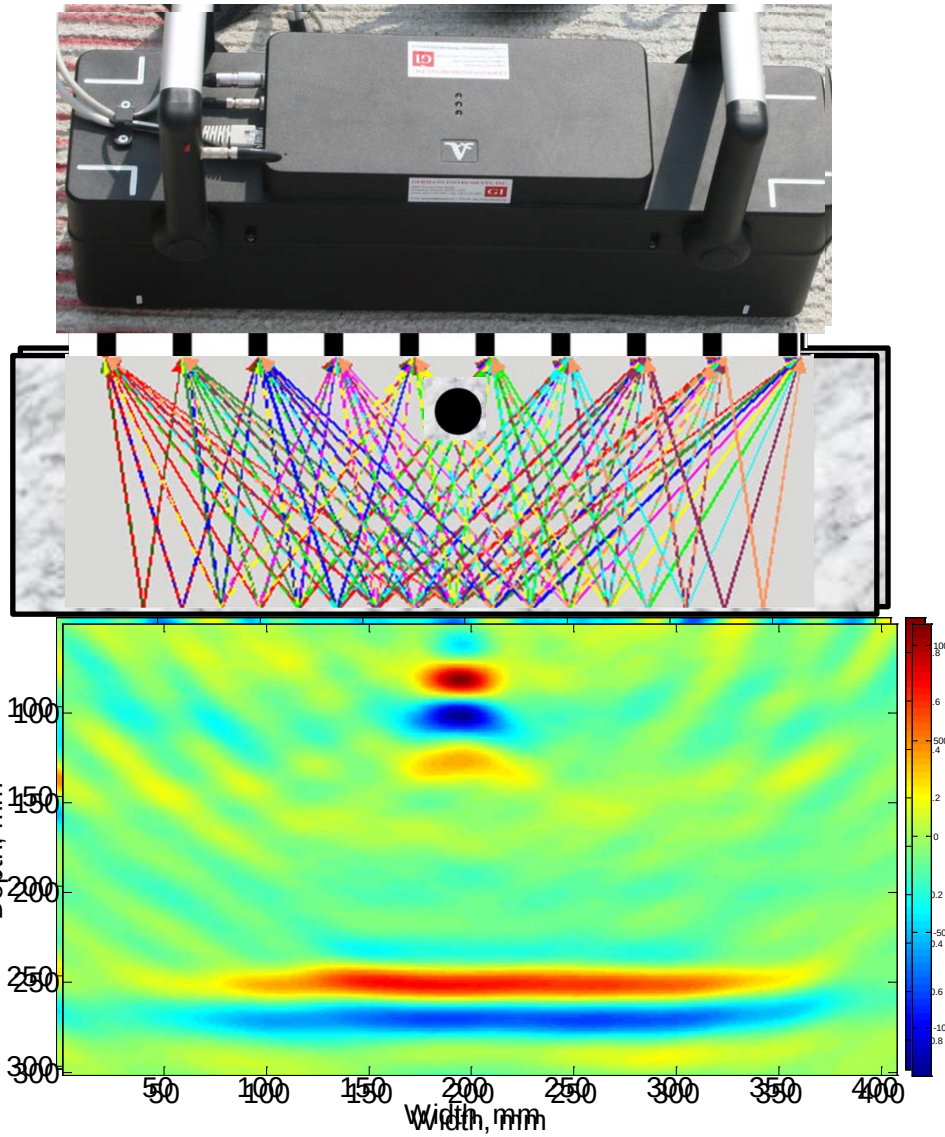

Reconstrução: Envelope (Amplitude Instantânea)

Transformação de Hilbert

$$\Upsilon(z) = \frac{1}{\pi} P \int_{-\infty}^{\infty} \frac{\chi(s)}{z-s} ds$$

Complex Signal

$$Z(z) = \chi(z) + j\,\Upsilon(z)$$

$$|Z(z)| = \sqrt{\chi(z)^2 + \Upsilon(z)^2}$$

P é o valor principal da integral simples

Cálculo do registro histórico do envelope

Oppenheim et al., 1989

$$\Psi_{e,r}^{IA}(t) = \sqrt{\left(\Psi_{e,r}(t)\right)^2 + \left(\frac{1}{\pi}\ P \int_{-\infty}^{\infty} \frac{\Psi_{e,r}(s)}{t-s} ds\right)^2}$$

Onde $\Psi_{e,r}^{IA}(t)$ define a amplitude instantânea do envelope do registro histórico do par, $\Psi_{e,r}(t)$

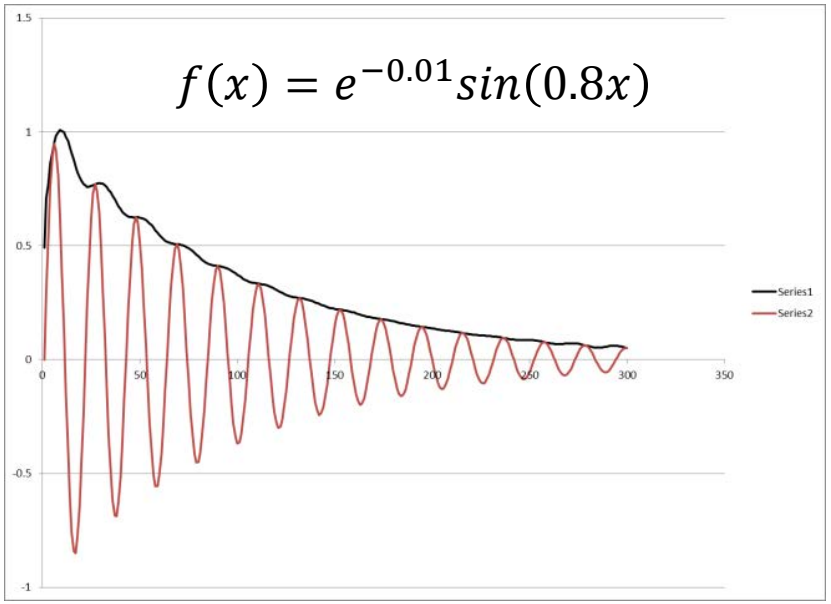

Reconstrução do Envelope

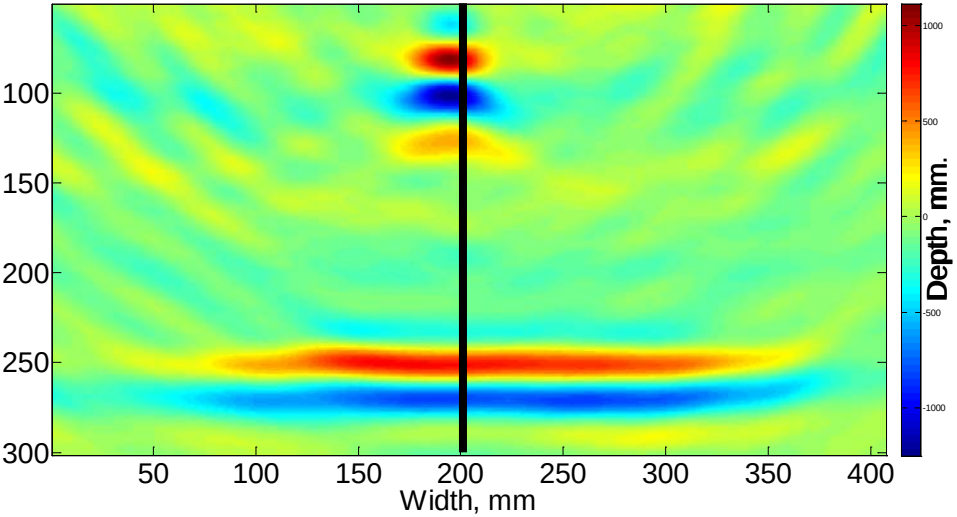

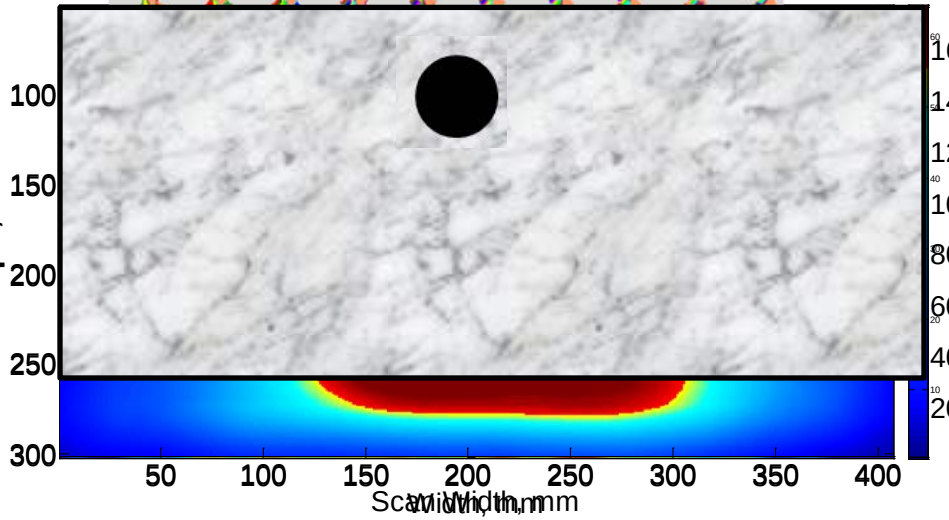

Hoegh and Khazanovich 2013

Limited Aperture Effect

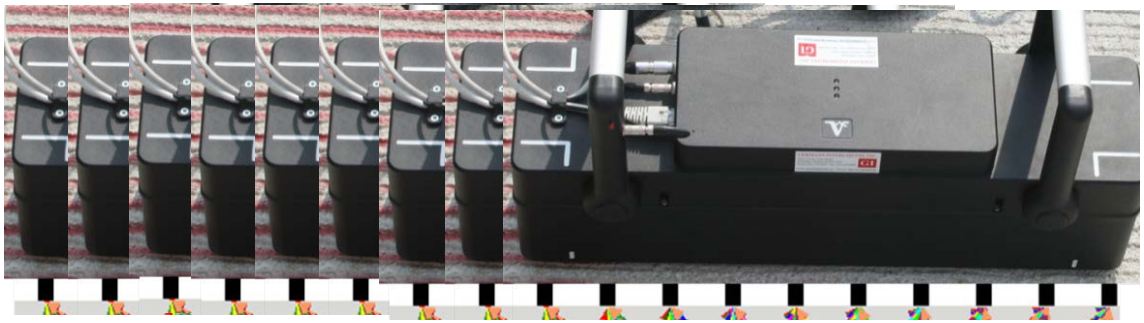

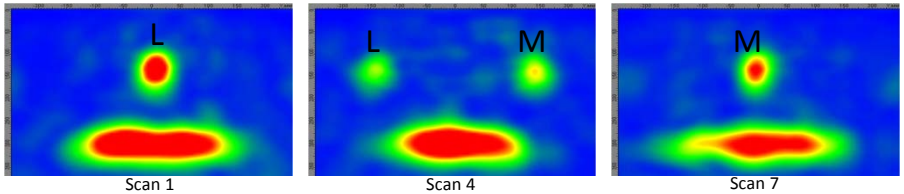

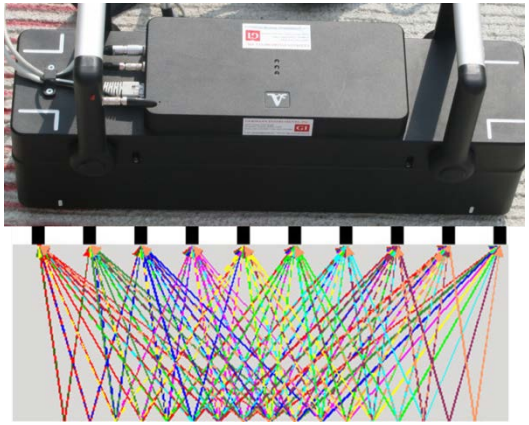

Expanded virtual array: SAFT Panoramic

$$[\hat{o}]^{PAN,m} = \begin{bmatrix} 0 & 0 & \hat{o}^{PAN,M}_{i^*,1} & \cdots & \hat{o}^{PAN,M}_{i^*+W-1,1} & 0 & 0 \\ 0 & 0 & \cdots & \hat{o}^{PAN,M}_{i,k} & \cdots & 0 & 0 \\ 0 & 0 & \cdots & \cdots & \cdots & 0 & 0 \\ 0 & 0 & \hat{o}^{PAN,M}_{i^*,D} & \cdots & \hat{o}^{PAN,M}_{W,D} & 0 & 0 \end{bmatrix}$$

$$\hat{o}^{PAN}_{k,i} = \max_{m}(\hat{o}^{EPAN,m}_{k,i}) \; for \; all \; k \; and \; i \; in \; the \; ROI_{PAN}$$

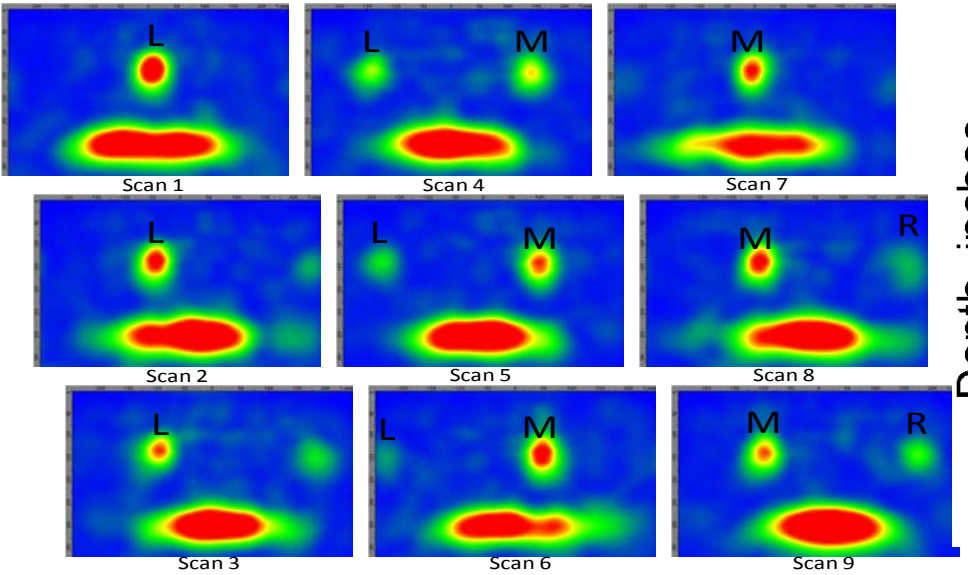

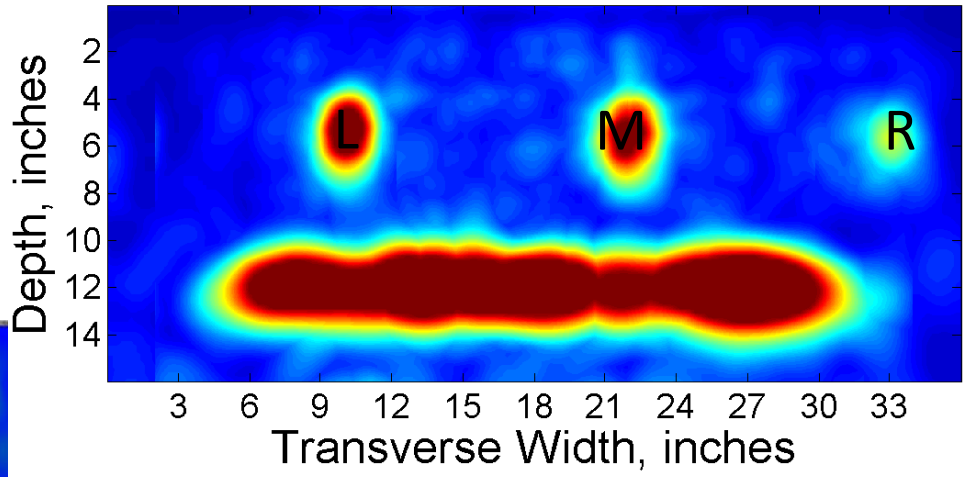

Effect of Uncertain Step Size

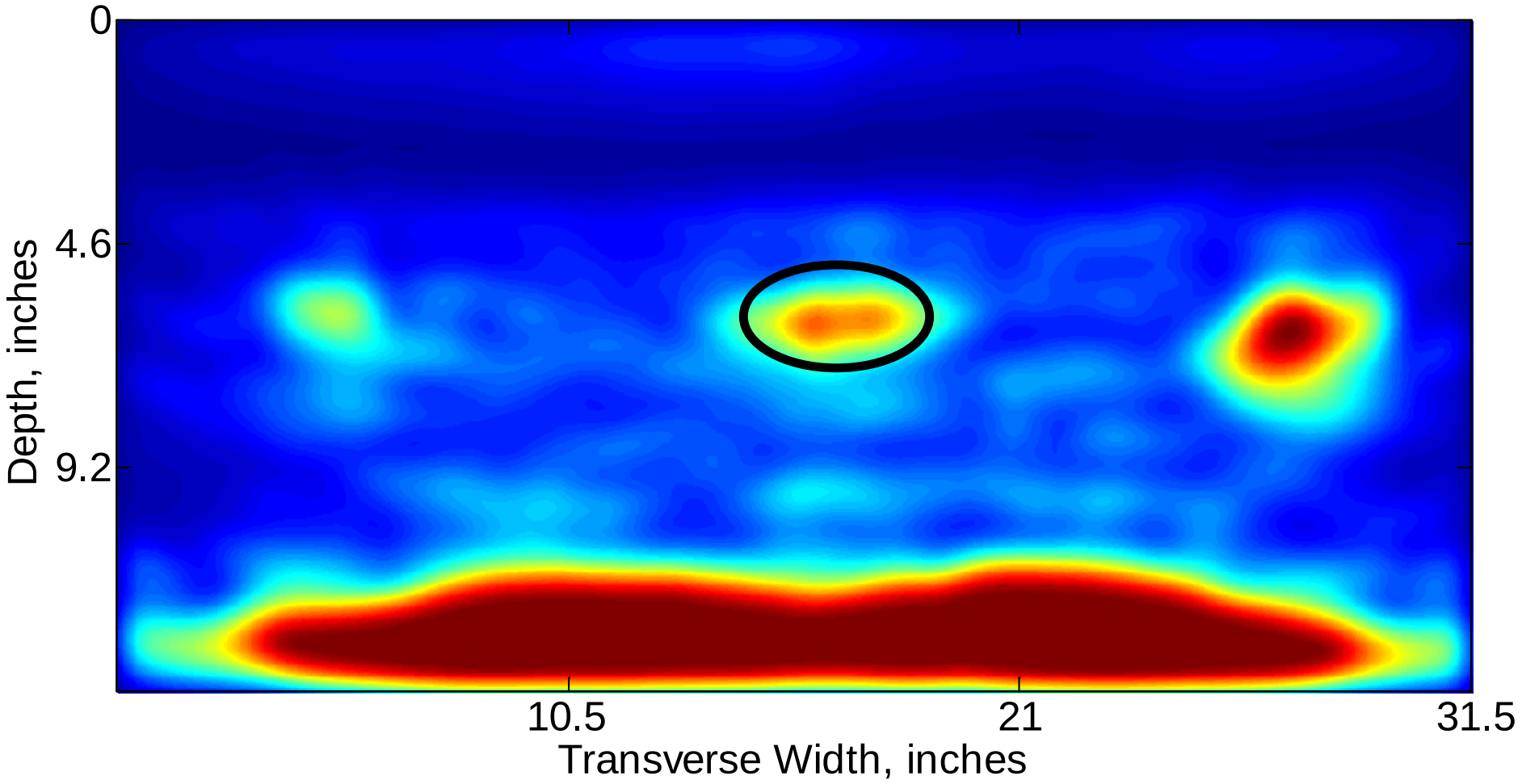

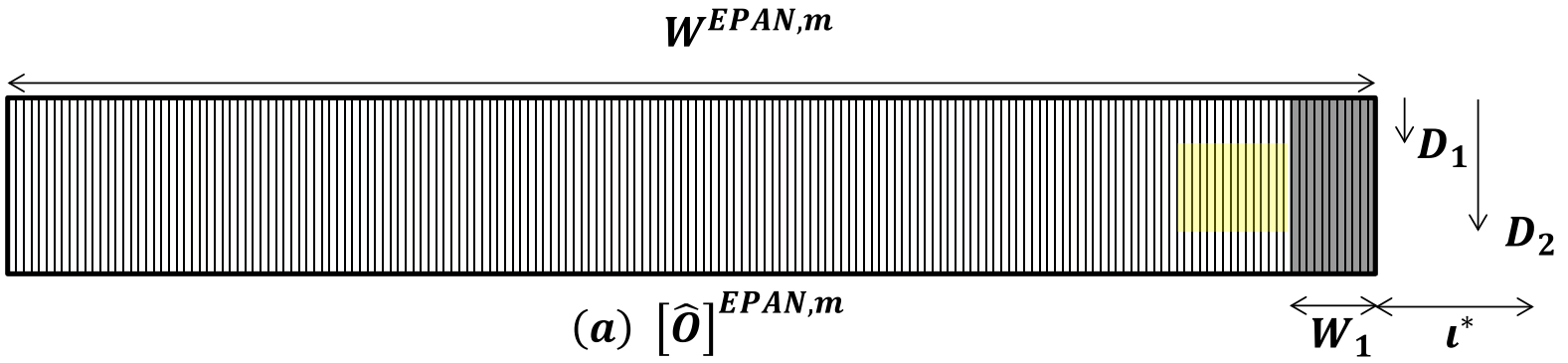

Para cada ι na faixa $[\iota_1, \iota_2]$

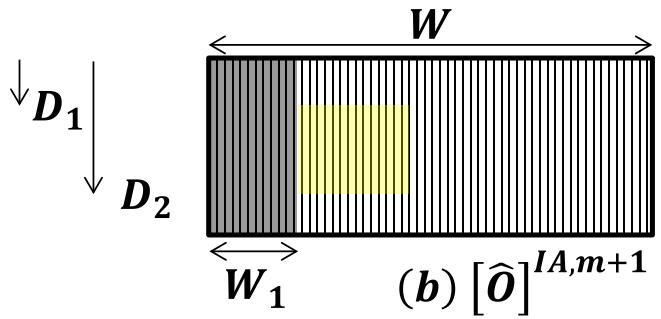

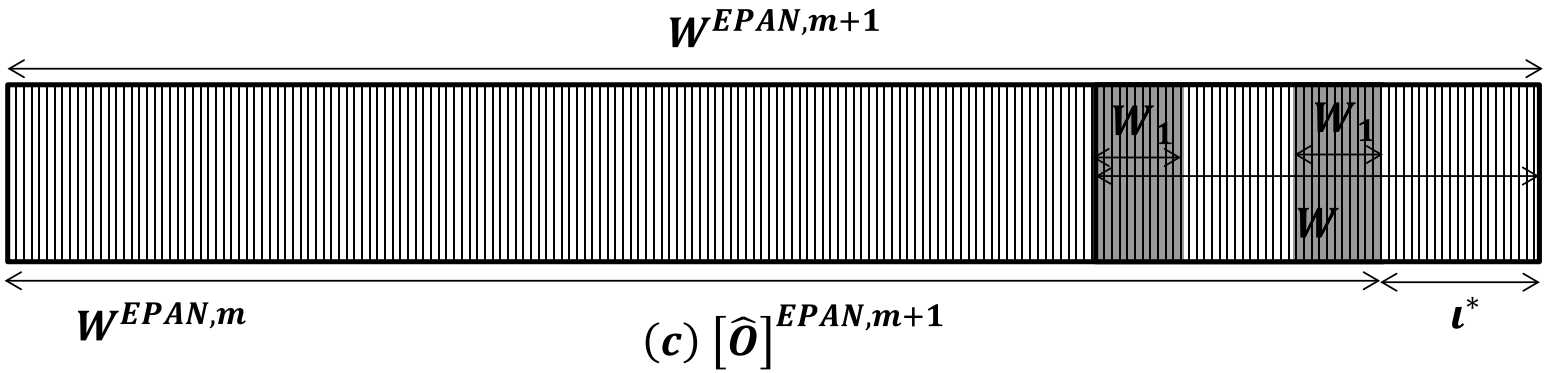

$$H(\iota) = \frac{\sum_{i=W_1+1}^{W-W_1-\iota} \sum_{k=D_1}^{D_2} \left(\hat{\boldsymbol{o}}^{EPAN,m}_{W^{EPAN,m}-W+\iota+i,k} - \hat{\boldsymbol{o}}^{EPAN,m}_{mean} \right) \left(\hat{\boldsymbol{o}}^{m+1}_{i,k} - \hat{\boldsymbol{o}}^{m+1}_{mean} \right)}{\sum_{i=W_1+1}^{W-W_1-\iota} \sum_{k=D_1}^{D_2} \left(\hat{\boldsymbol{o}}^{EPAN,m}_{W^{EPAN,m}-W+\iota+i,k} - \hat{\boldsymbol{o}}^{EPAN,m}_{mean} \right)^2 \sum_{i=W_1+1}^{W-W_1-\iota} \sum_{k=D_1}^{D_2} \left(\hat{\boldsymbol{o}}^{m+1}_{i,k} - \hat{\boldsymbol{o}}^{m+1}_{mean} \right)^2}$$

$$\hat{\boldsymbol{o}}^{EPAN,m}_{mean} = \frac{\sum_{i=W^{EPAN,m}-W_1}^{W^{EPAN,m}-W+\iota+W_1+1} \sum_{k=D_1}^{D_2} \hat{\boldsymbol{o}}^{EPAN,m}_{i,k}}{(W - 2W_1 - \iota)(D_2 - D_1 + 1)}$$

ι na faixa $[\iota_1, \iota_2]$

$$\hat{\boldsymbol{o}}^{m+1}_{mean} = \frac{\sum_{i=W_1+1}^{W-W_1-\iota} \sum_{k=D_1}^{D_2} \hat{\boldsymbol{o}}^{m+1}_{i,k}}{(W - 2W_1 - \iota)(D_2 - D_1 + 1)}$$

$$\hat{\boldsymbol{O}}^{EPAN,m+1}_{i,k} = \hat{\boldsymbol{O}}^{EPAN,m}_{i,k} \; for \; i < W^{EPAN,m} - W + \iota^* + W_1$$

$$\hat{\boldsymbol{O}}^{EPAN,m+1}_{i,k} = max\left(\hat{\boldsymbol{O}}^{EPAN,m}_{i,k}, \hat{\boldsymbol{O}}^{m+1}_{i-W^{EPAN,m}+W-\iota^*,k} \right) \text{ for } W^{EPAN,m} < i \leq W^{EPAN,m+1}$$

$H(\iota)$

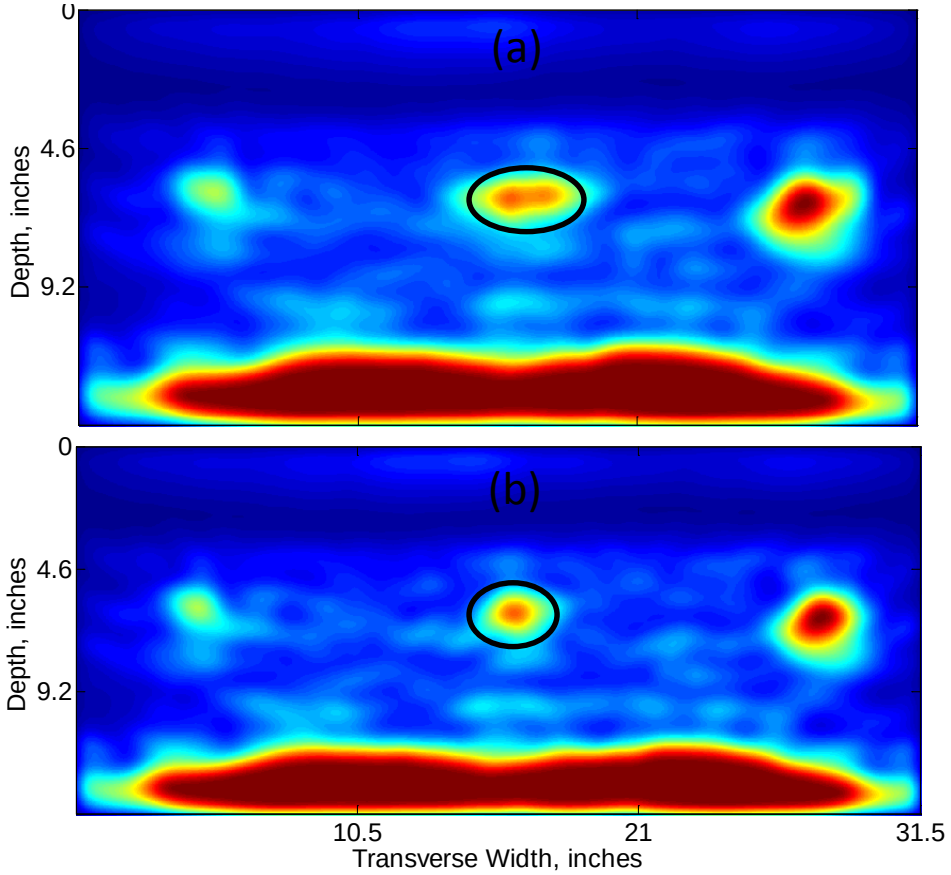
(a)
(b)
Depth, inches
0
4.6
9.2
10.5
21
31.5
Transverse Width, inches

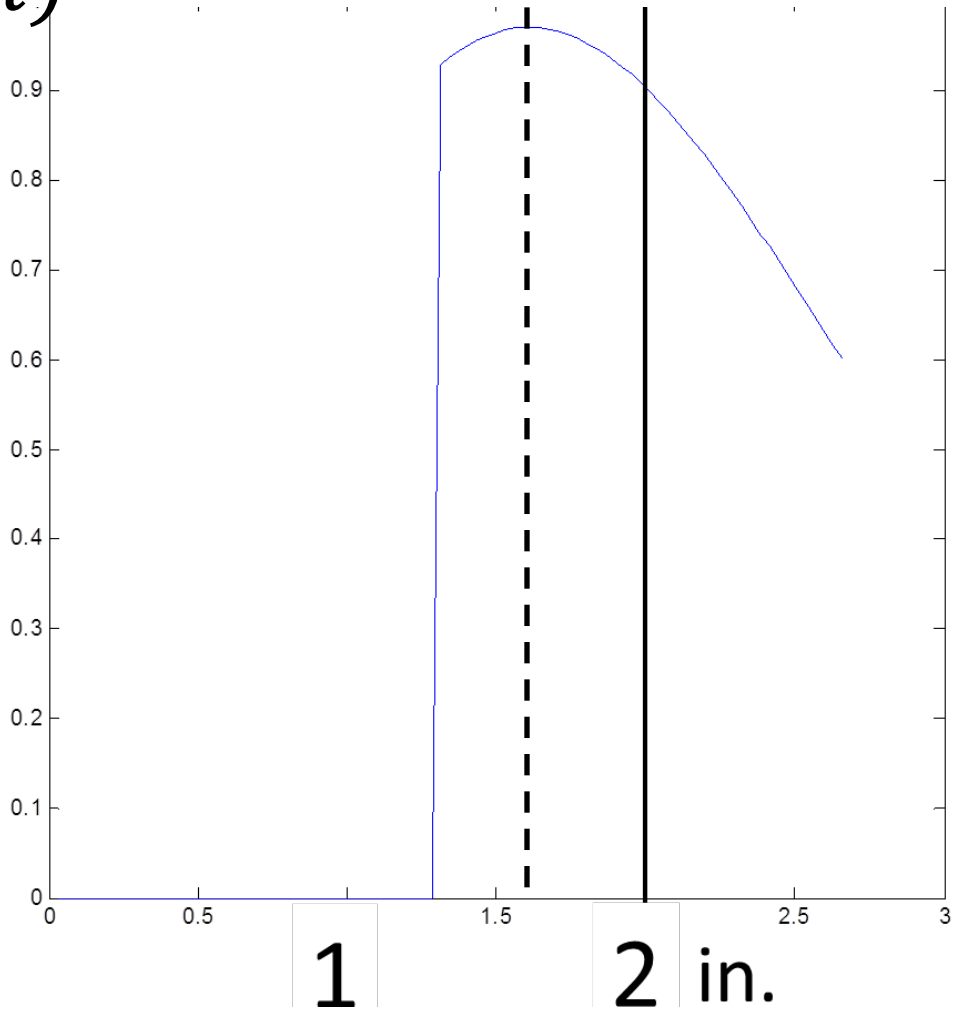
0.9
0.8
0.7
0.6
0.5
0.4
0.3
0.2
0.1
0
0.5
1.5
2.5
3
1
2
in.

Aplicacoes

Queremos o extensor de Minnesota para o MIRA!

Anne Beeldens, Belgian Road Research Centre

Applications

- Espessuras de Pavimentos de Concreto
- Posicao de armaduras, barras de transferencia de carga e barras de ligacao
- Posicao de delaminacoes
- Degradacao subsuperficial
- Adensamento inadequado do concreto, “bicheiras”, torroes de argila, etc.
- Degradacao das juntas de pavimentos
- Aderencia do aco ao concreto

Concrete Thickness

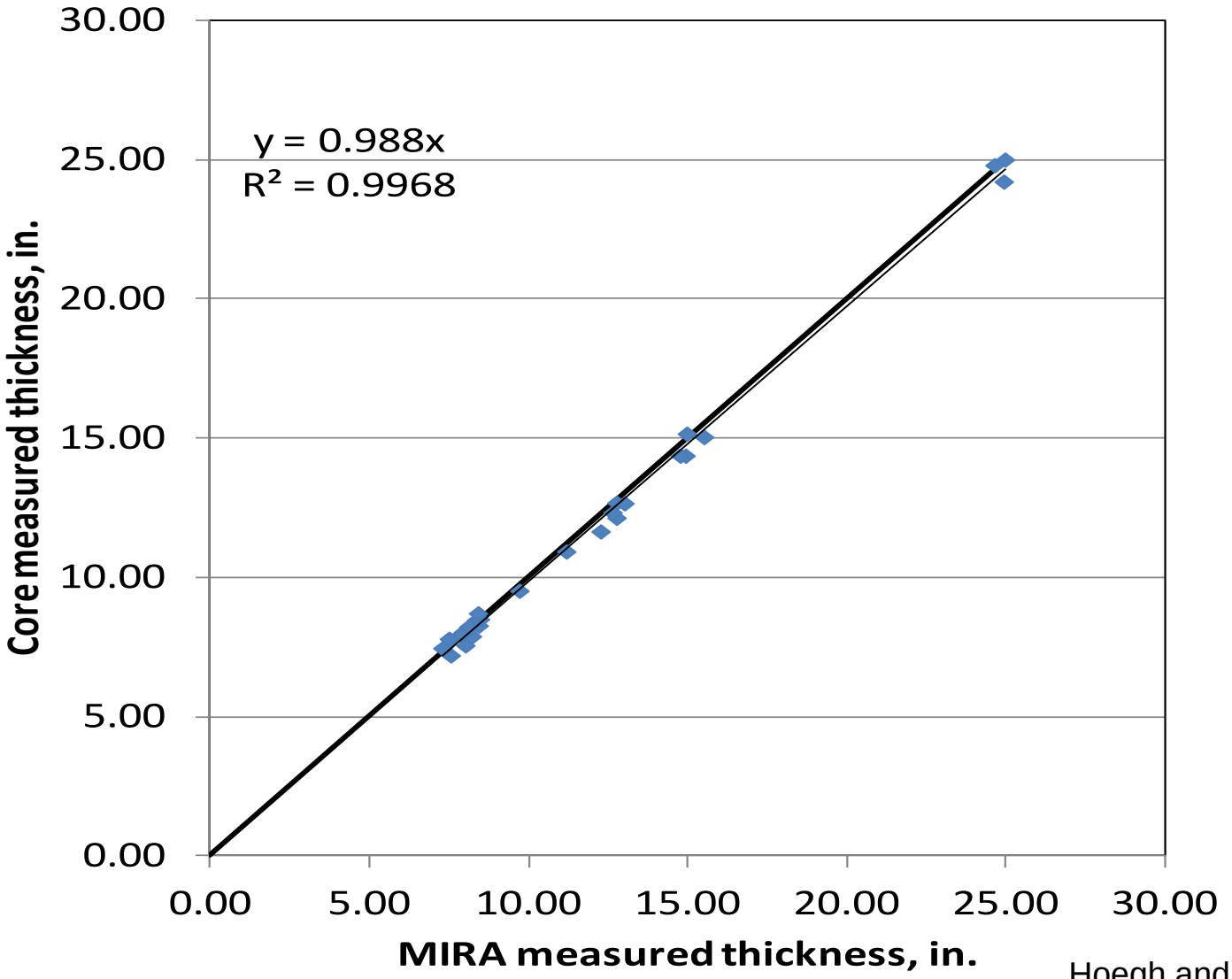

Hoegh and Khazanovich, TRB 2014

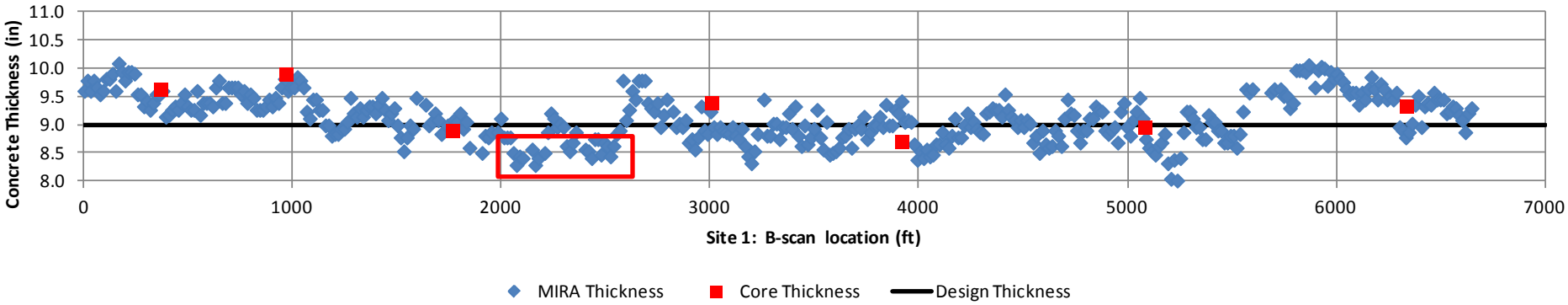

Mais de 400 medidas em menos de uma hora

- Interpretação automatizada
- Sem necessidade de calibração adicional
- Boa concordância com amostras extraidas
- Variacoes em espessuras

Vancura et al, TRR 2013

Reinforcement Location

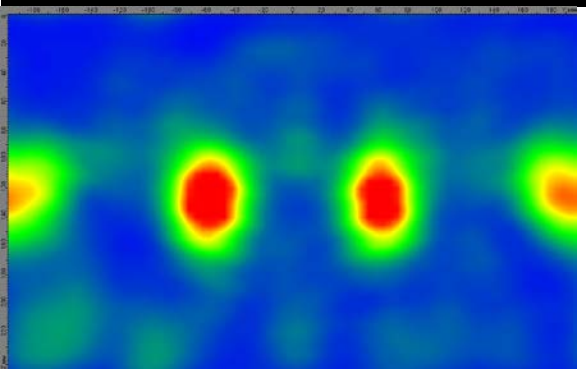

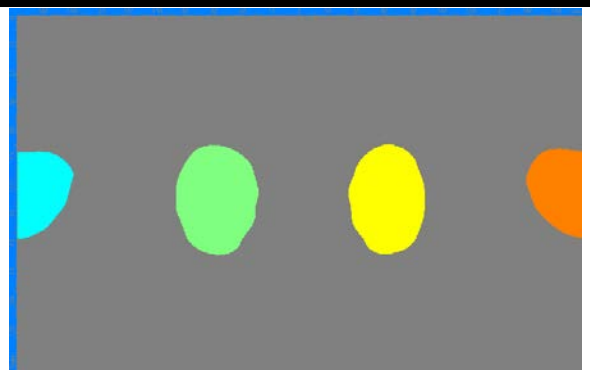

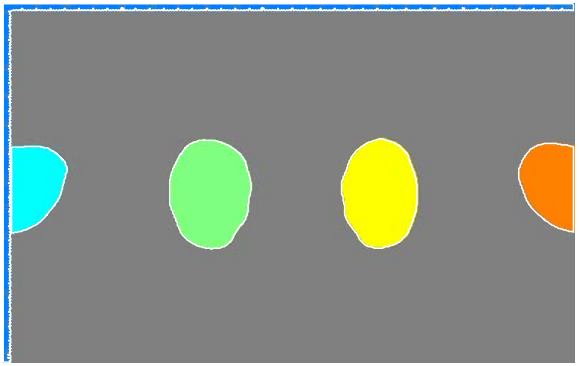

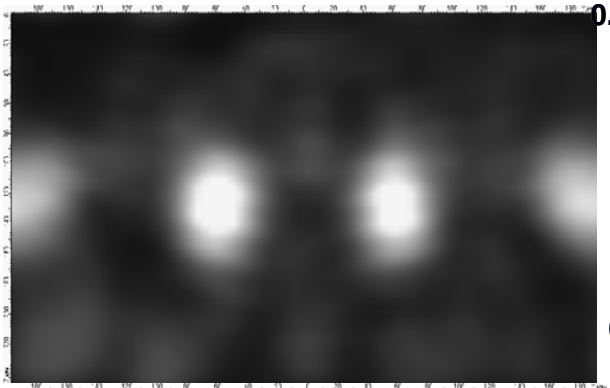

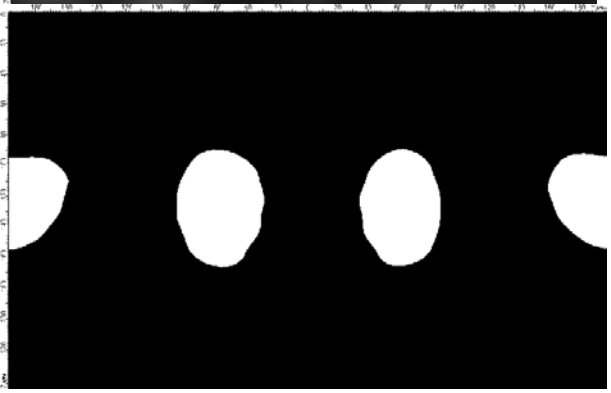

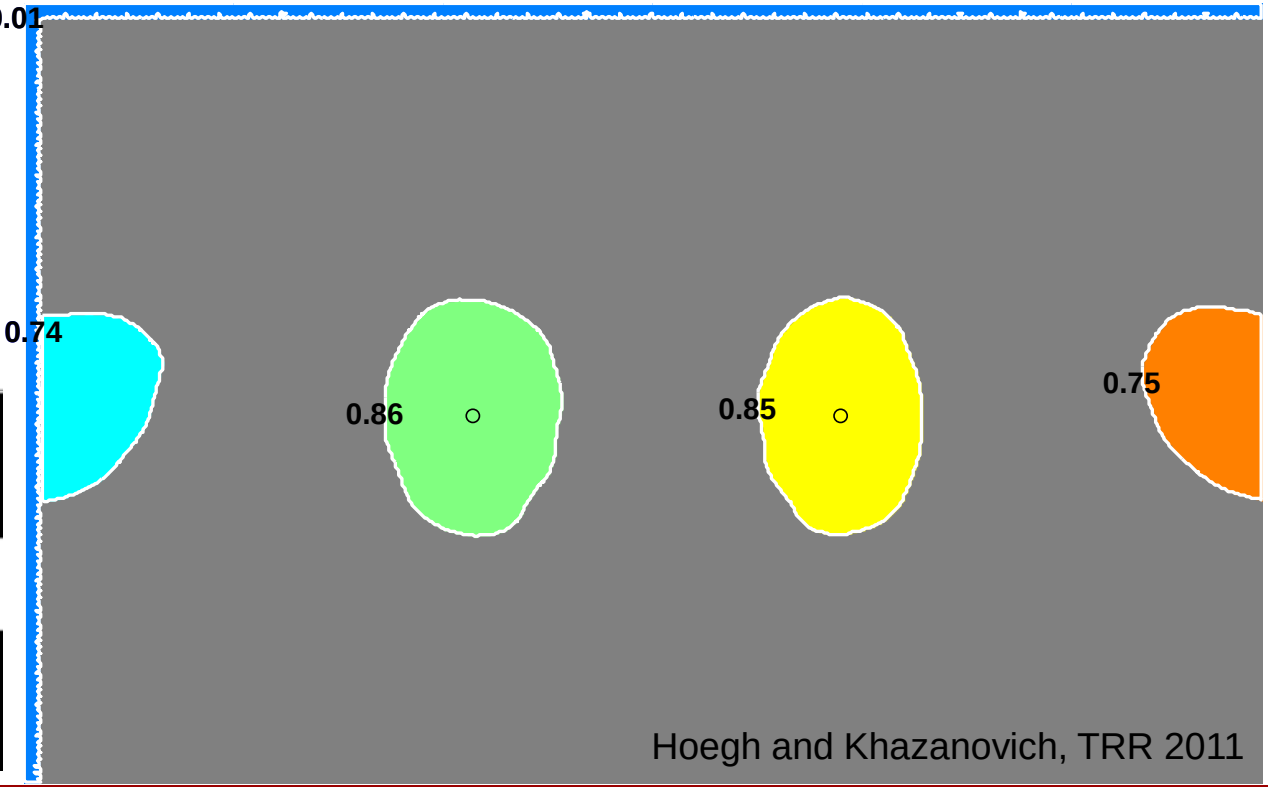

Hoegh and Khazanovich, TRR 2011

MIRA vs Core Concrete Cover

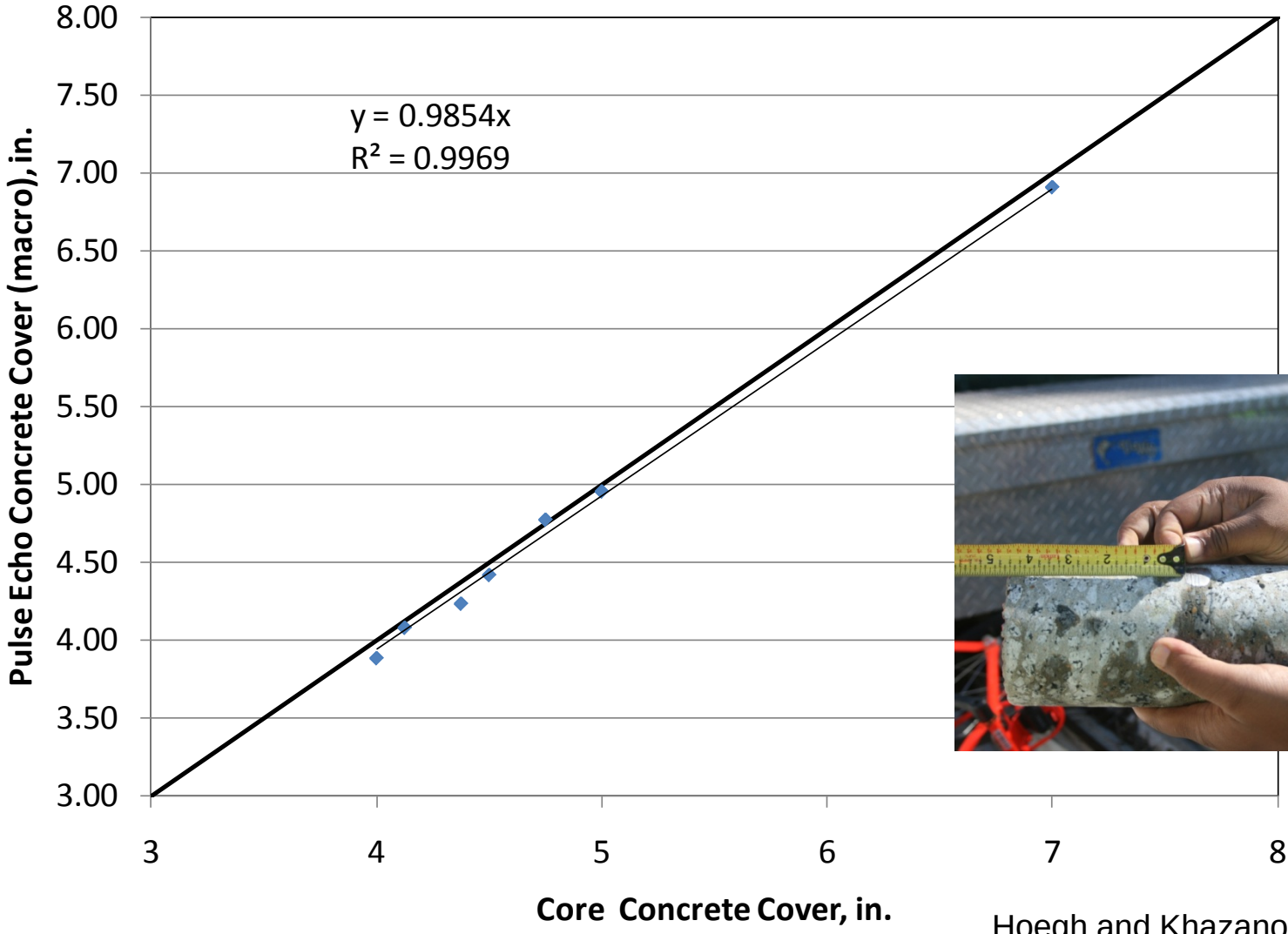

Hoegh and Khazanovich, TRR 2011

Measurements of pavement thickness and longitudinal rebar concrete cover for project (about 5 km of testing in 15 m intervals).

Field Application – Atlanta Georgia CRCP

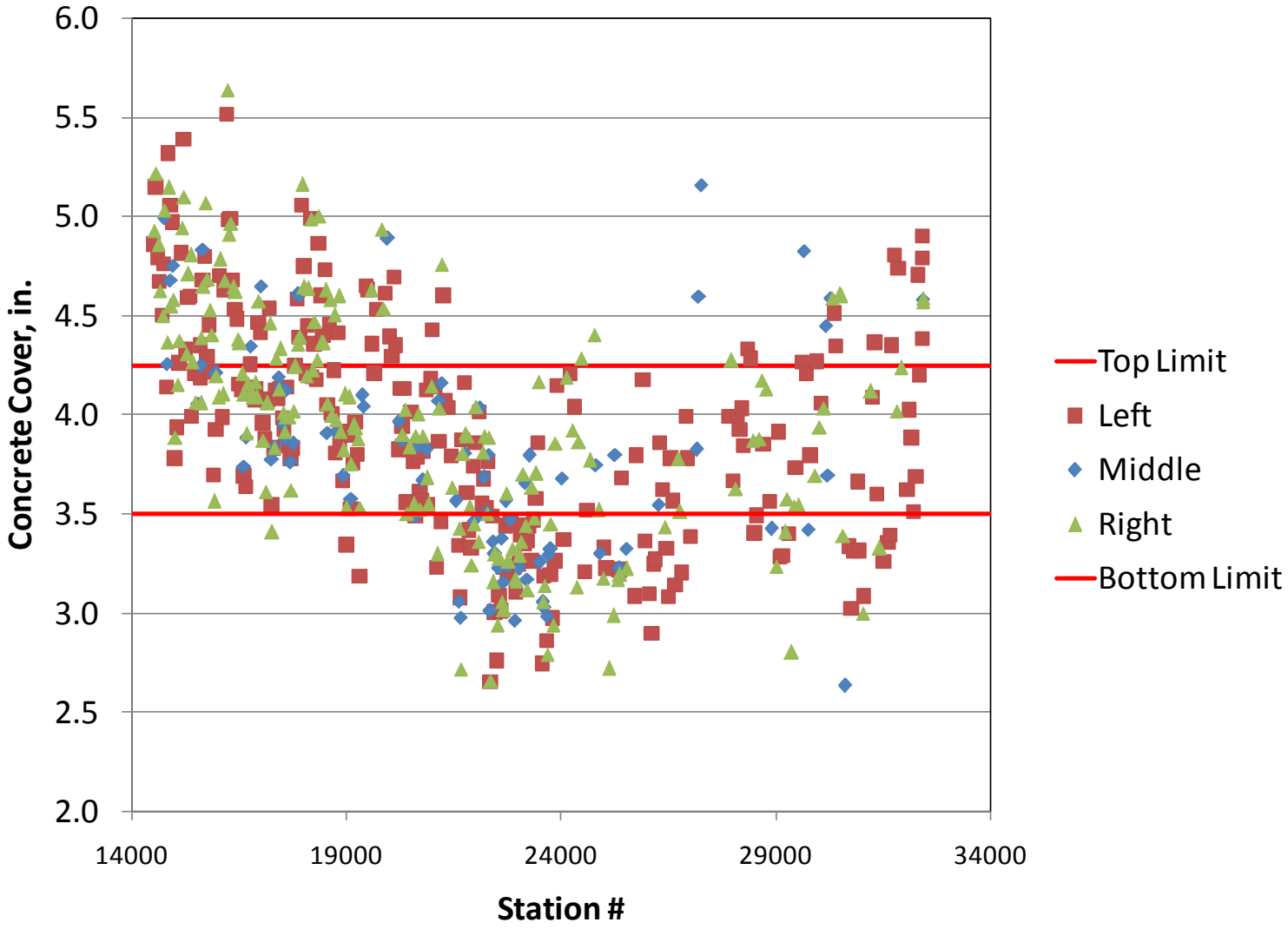

Delamination Mapping

Antwerpen, Belgium. Continuously Reinforced Concrete

Not Delaminated

Delaminated

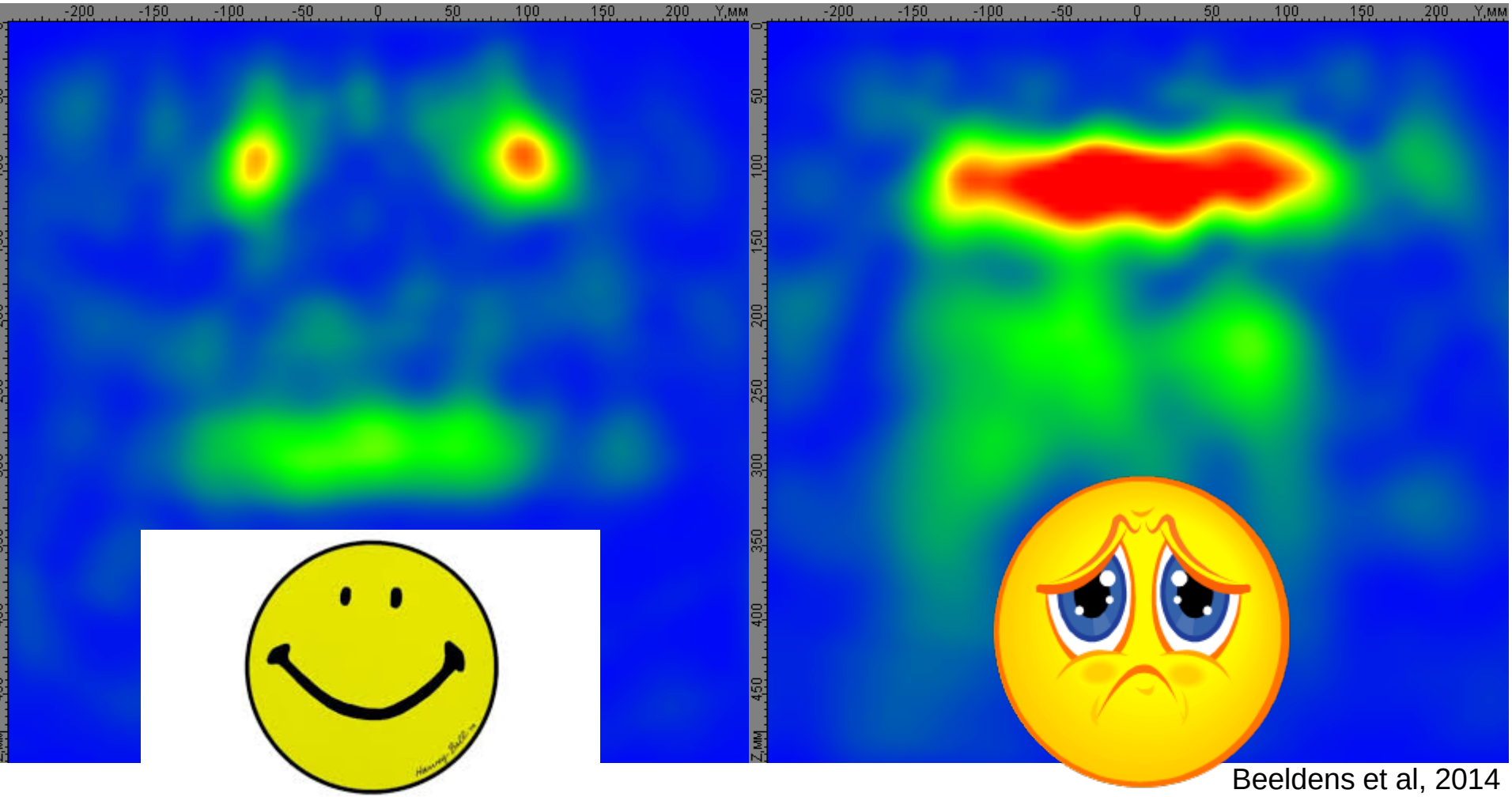

Beeldens et al, 2014

Análise de Tomográfica Ultrassônica de Dados (UTSA) usando Correlação de Pearson

$$C^{IA,m} = \frac{Cov\left[\left[\hat{\boldsymbol{O}}\right]^{IA,ref}, \left[\hat{\boldsymbol{O}}\right]^{IA,m}\right]}{\sqrt{Var\left[\left[\hat{\boldsymbol{O}}\right]^{IA,ref}\right] Var\left[\left[\hat{\boldsymbol{O}}\right]^{IA,m}\right]}}$$

$$= \frac{\sum_{i=1}^{W}\sum_{k=1}^{D}\left(\hat{\boldsymbol{o}}_{i,k}^{IA,ref} - \hat{\boldsymbol{o}}_{mean}^{IA,ref}\right)\left(\hat{\boldsymbol{o}}_{i,k}^{IA,m} - \hat{\boldsymbol{o}}_{mean}^{IA,m}\right)}{\sum_{i=1}^{W}\sum_{k=1}^{D}\left(\hat{\boldsymbol{o}}_{i,k}^{IA,ref} - \hat{\boldsymbol{o}}_{mean}^{IA,ref}\right)^2 \sum_{i=1}^{W}\sum_{k=1}^{D}\left(\hat{\boldsymbol{o}}_{i,k}^{IA} - \hat{\boldsymbol{o}}_{me}^{IA}\right.}$$

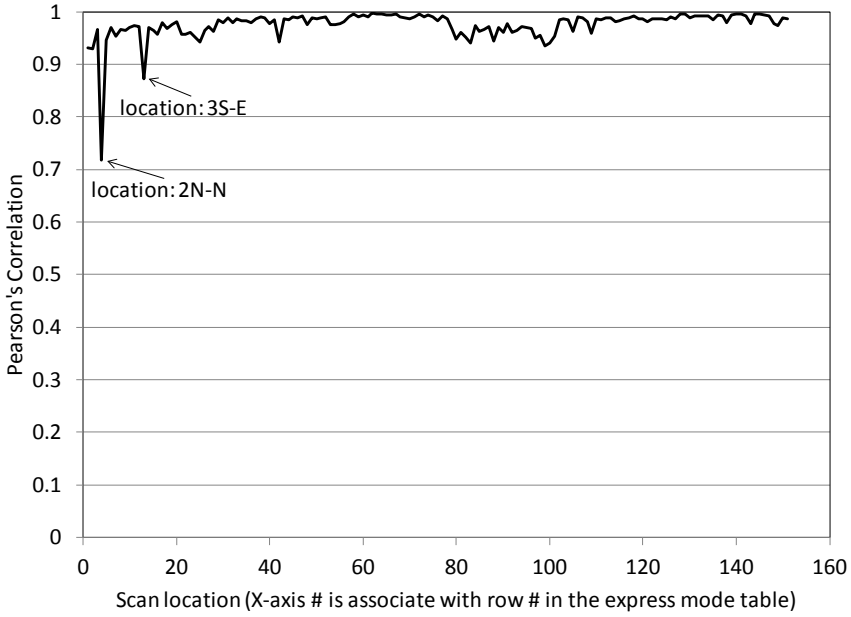

$\left[\hat{\boldsymbol{O}}\right]^{IAref}$ and $\left[\hat{\boldsymbol{O}}\right]^{IA,m}$ são as matrizes para a referência e *m*-ésima SAFT-IA B-scan

Hoegh and Khazanovich, ASTM JTE 2012

Correllelogram of Concrete without Damage

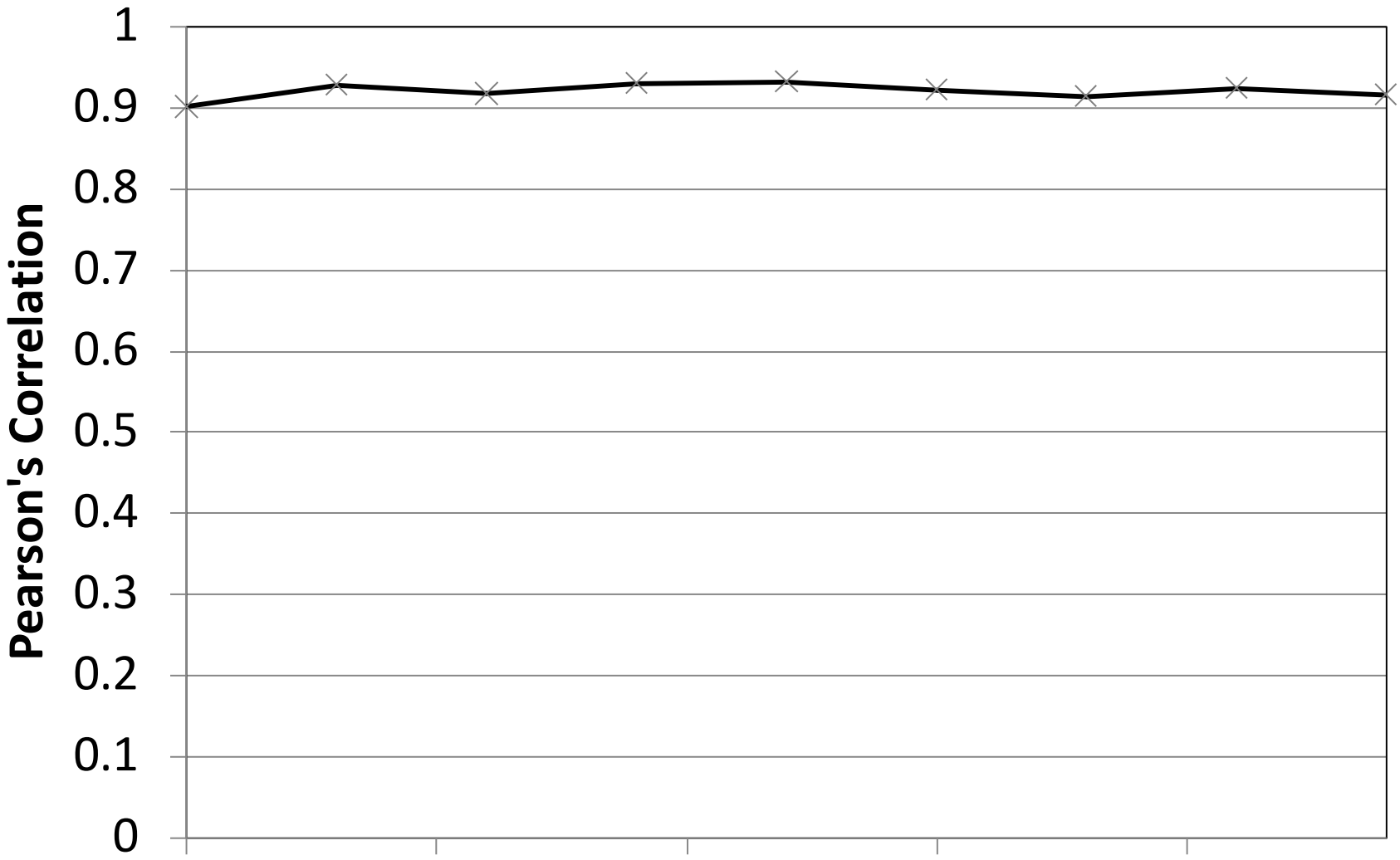

Correllelogram of Concrete with Defects

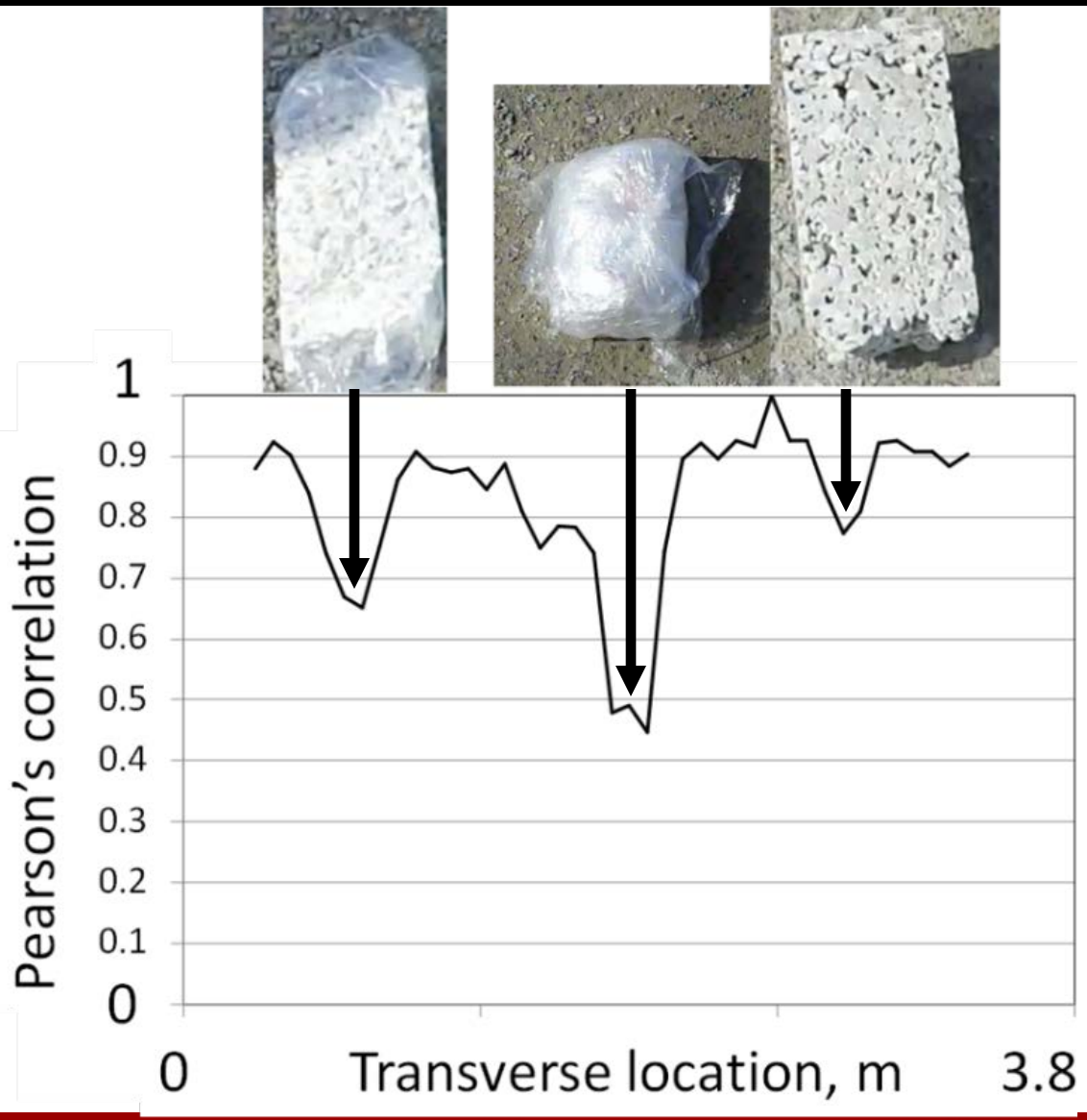

Zoomed –in View, Leftmost Fabricated Defect

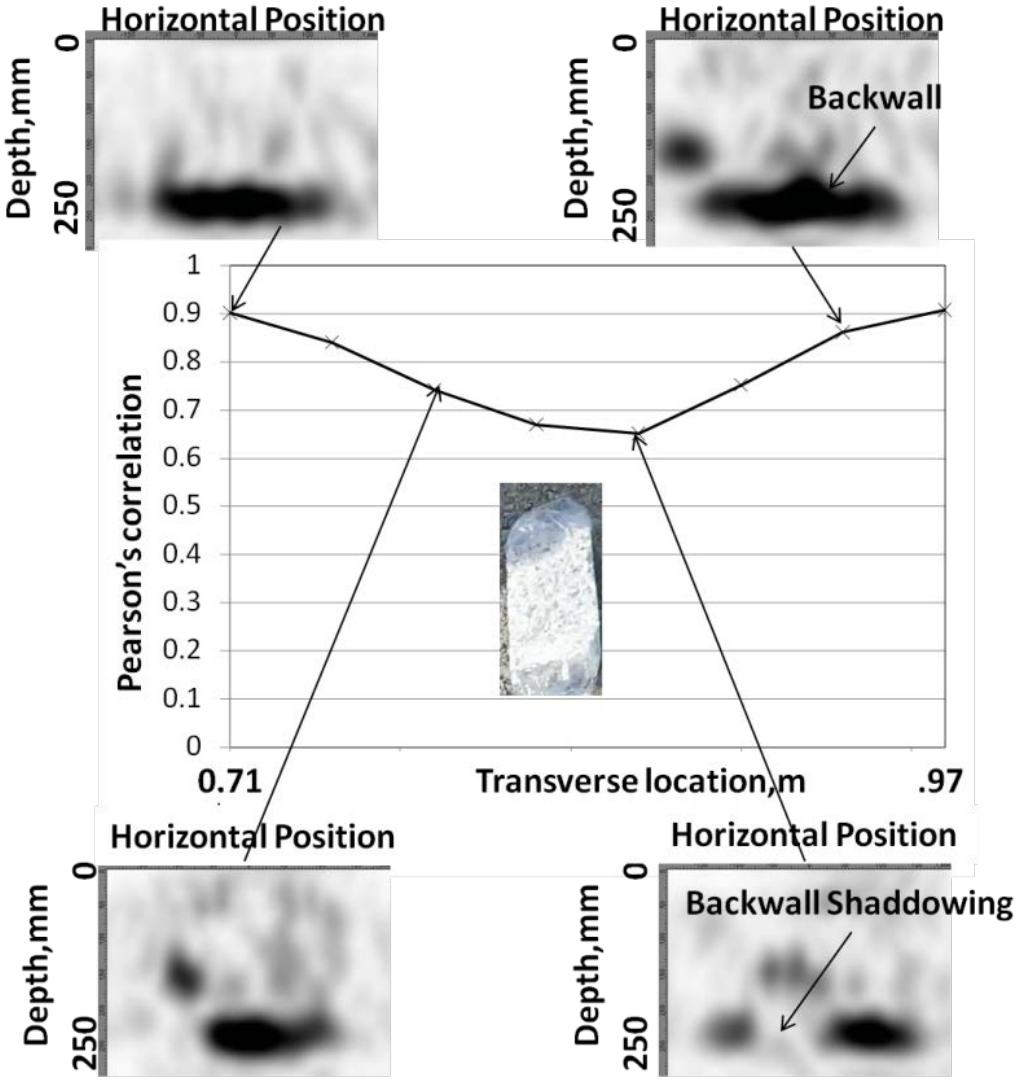

Conclusions

- Diagnostico nao-destrutivo de estruturas de concreto e um problema importante e cheio de desafios
- Melhorias feitas no equipamento MIRA tornou possivel a avaliacao quantitativa de condicoes subsuperficiais
- *Generalized Kirchoff migration-based synthetic aperture focusing technique* (SAFT) para reconstrucao e demais tecnicas associadas sao ferramentas promissoras para a solucao de problemas praticos